FACULTY OF PHARMACEUTICAL SCIENCES

IN VITRO LIVER-TARGETED LIPID NANOPARTICLES WITH APOLIPOPROTEIN E AND N-ACETYL-GALACTOSAMINE

Jonie Verdonck

A Master dissertation for the study programme Master in Drug Development

Academic year: 2022 – 2023

GHENT UNIVERSITY

UMC Utrecht

ABSTRACT

Hoping to find a new perspective on the treatment of atherosclerosis, the influence of ceramide was investigated. Since ceramide contributes to the evolution of atherosclerosis, interrupting ceramide synthesis could lead to a possible treatment for the disease. One potential approach is to silence genes encoding for enzymes in the de novo synthesis of ceramide. Genes that are interesting to silence for this purpose are CerS and DEGS, two key enzymes in the ceramide pathway.

For gene silencing, nucleic acid therapeutics such as siRNA are well suited. siRNA is too unstable to administer as such, which is why lipid nanoparticles (LNPs) are used as delivery vehicles. Since ceramide is mainly synthesised in hepatocytes, the aim is to develop LNPs that target hepatocytes. Hepatocytes can be specifically targeted using two different approaches, apolipoprotein E (Apo E) and N-acetyl-galactosamine (GalNAc). Apo E binds specifically to the low-density lipoprotein receptor (LDLR) and GalNAc to the asialoglycoprotein receptor (ASGPR), both highly expressed on hepatocytes. This ligand-receptor interaction could lead to targeted LNP uptake and transfection in the specific target cells.

The aim of this paper was to investigate whether LNPs conjugated to Apo E and GalNAc manage to specifically target the hepatocytes. A hepatocarcinoma cell line, HepG2, was used to test in vitro hepatocyte targeting, as they highly express both LDLR and ASGPR 1. HEK293FT cells were used as a negative control cell line with low expression of LDLR and no ASGPR 1 expression. Both cell lines were first transfected with both Apo E LNPs and GalNAc LNPs with molar ratios of GalNAc ranging from 0.05% to 1%, all encapsulated with Cy 5-labelled eGFP mRNA. The GalNAc LNPs were made by both adding the GalNAc to the lipid phase and post-inserting the group onto the LNP. The Apo E LNPs showed a significant positive targeting result compared to the non-targeted LNPs. GalNAc-targeting showed no improvement in HepG2 cells. In a later step, siRNA was encapsulated in the LNPs to demonstrate targeted silencing. Apo E LNPs managed to demonstrate additional silencing in HepG2 cells compared to the non-targeted variant. GalNAc LNPs barely lead to additional silencing of genes.

SAMENVATTING

Hopend op het vinden van een nieuw perspectief voor de behandeling van atherosclerose, werd de invloed van ceramide onderzocht. Aangezien ceramide bijdraagt aan de ontwikkeling van atherosclerose, zou het onderbreken van de ceramidesynthese kunnen leiden tot een mogelijke behandeling van de ziekte. Een potentiële aanpak is het stilleggen van genen die coderen voor enzymen in de de novo synthese van ceramide. Genen die interessant zijn om voor dit doel stil te leggen zijn CerS en DEGS, twee sleutelenzymen in de ceramide pathway.

Voor het stilleggen van genen zijn nucleïnezuur therapeutica zoals siRNA zeer geschikt. siRNA is te onstabiel om als dusdanig toe te dienen, daarom worden lipide nanodeeltjes (LNPs) gebruikt als toedieningsmiddel. Aangezien ceramide vooral in de hepatocyten wordt gesynthetiseerd, is het doel LNPs te ontwikkelen die gericht zijn op hepatocyten. Hepatocyten kunnen specifiek worden getarget met behulp van twee verschillende benaderingen, apolipoproteine E (Apo E) en N-acetyl-galactosamine (GalNAc). Apo E bindt specifiek aan de low-density lipoproteïne receptor (LDLR) en GalNAc aan de asialoglycoproteïne receptor (ASGPR), die beide sterk tot expressie komen op hepatocyten. Deze ligand-receptor interactie zou kunnen leiden tot gerichte LNP opname en transfectie in de specifieke doelcellen.

Het doel van dit artikel was na te gaan of LNPs geconjugeerd met Apo E en GalNAc erin slagen zich specifiek op de hepatocyten te richten. Een hepatocarcinoom cellijn, HepG2, werd gebruikt om de in vitro hepatocyten targeting te testen, aangezien zij zowel LDLR als ASGPR 1 in hoge mate tot expressie brengen. HEK293FT-cellen werden gebruikt als negatieve controlecellijn met lage expressie van LDLR en zonder ASGPR 1 expressie. Beide cellijnen werden eerst getransfecteerd met zowel Apo E LNPs als GalNAc LNPs met molaire verhoudingen van GalNAc variërend van 0,05% tot 1%, allen met Cy 5 gelabeld eGFP mRNA ingekapseld. De GalNAc LNPs werden gemaakt door zowel het GalNAc aan de lipidenfase toe te voegen als de groep achteraf op het LNP te plaatsen. De Apo E LNPs toonden een significant positief getarget resultaat in vergelijking met de niet-getargete LNPs. De GalNAc-targeting gaf geen verbetering in de HepG2-cellen. In een latere stap werd siRNA ingekapseld in de LNPs om gerichte silencing aan te tonen. Apo E LNPs slaagden erin een additionele silencing in HepG2-cellen aan te tonen in vergelijking met de niet-getargete variant. GalNAc LNP's leidden amper tot een bijkomende uitschakeling van genen.

ACKNOWLEDGEMENTS

I would like to start by thanking professor Koen Raemdonck (Ghent University) and professor Raymond Schiffelers (UMC Utrecht) to give me the opportunity to work in research abroad. Especially prof. Schiffelers for supporting me and helping me through my journey. I benefited greatly from the advice you gave me, for my period there as well as for the future.

I would like to express my gratitude for Arnold Koekman for being my supervisor through the last part of my internship. Thank you for always making time for me and helping me in every way you could. I really appreciate having you as my teacher.

Thank you to Yanjuan Xu and Pol Escudé Martinez de Castilla for helping me in the first part of my internship and guiding me through my first experiments.

Zoë Eeckhout, thank you for being there for me throughout this whole experience inside as well as outside of the lab. Thank you for always supporting me, motivating me and taking care of me. I will miss my daily cooking buddy but I am excited for the new memories the future holds for us.

Thank you to Anil Kumar Deschantri and Maria Laura Tognoli for guiding me through some experiments. I really appreciate taking the time out of your day to explain the details of certain experiments with me.

I would also like to thank the other students in the lab and in particular Raul Leandro, Mafalda Cabana, Tanya Karakyriakou and Maryse Boesveld. Thank you for lighting up my days in the lab and all the memories outside of it.

Also a big thank you to the other members of the CDL (UMC Utrecht) for creating such a nice environment to work in.

Thank you to the people living in the Biltstraat residency with me for making the past few months so memorable and all the memories we share. I can not wait to continue our friendships.

Lastly, I want to thank my parents and brother for all the support they gave me and for motivating me to achieve my goals.

TABLE OF CONTENT

ABBREVIATIONS

ACE	Angiotensin Converting Enzyme
Ago 2	Argonaut 2 protein
ANOVA	Analysis of variance
APC	Allophycocyanin
Apo E	Apolipoprotein E
AR	Androgen receptor
ASGPR	Asialoglycoprotein receptor
ASO	Antisense oligonucleotide
BSA	Bovine serum albumin
CDL	Central Diagnostic Laboratory
cDNA	copy DNA
CerS	Ceramide synthase
Cq	Quantification cycle
Cy 5	Cyanine 5
DEGS	Dihydroceramide desaturase
Demiwater	Demineralised water
DLin-MC3-DMA	4-(dimethylamino)-butanoic acid, (10Z,13Z)-1-(9Z,12Z)-9,12-octadecadien-1-yl-10,13-nonadecadien-1-yl ester
DLS	Dynamic light scattering
DMEM	Dulbecco's Modified Eagle Medium
DMG-PEG2000	1,2-dimyristoyl-rac-glycero-3-methoxypolyethylene glycol-2000
DMSO	Dimethyl sulfoxide
DNA	Deoxyribonucleic acids
DPBS	Dulbecco’s Phosphate Buffered Saline
DSPC	1,2-Distearoyl-sn-glycero-3-phosphocholine
dsRNA	Double-stranded RNA
DTT	Dithiothreitol
EDTA	Ethylenediaminetetraacetic acid
eGFP	Enhanced Green Fluorescent Protein
FACS	Fluorescence activated cell sorting
FCS	Fetal calf serum
FITC	Fluorescein isothiocyanate

Fw	Forward
GalNAc	N-acetyl-galactosamine
GalNAc-PEG	1,2-distearoyl-sn-glycero-3-phosphoethanolamine-N-[tris-GalNAc-GABA-(polyethylene glycol)-2000]
GAPDH	Glyceraldehyde 3-phosphate dehydrogenase
GlcNAc	N-acetyl-glucosamine
HDL	High-density lipoprotein
HEK	Human Embryonal Kidney
HEPES	4-(2-hydroxyethyl)piperazin-1-ylethanesulphonic acid
HMG-CoA	3-hydroxy-3-methylglutaryl-CoA
kDa	kilo Dalton
KDSR	3-ketosphinganine reductase
LDL	Low-density lipoprotein
LDLR	Low-density lipoprotein receptor
LNP	Lipid nanoparticle
MHF	Microfluidic hydrodynamic focusing
MOPS	3-(N-morpholino)propanesulfonic acid
mRNA	messenger RNA
N/P ratio	Nitrogen-to-phosphate ratio
NA	Nucleic acids
NAT	Nucleic acid therapeutics
NT	Non-targeted
PBS	Phosphate Buffered Saline
PCR	Polymerase chain reaction
PCSK9	Proprotein convertase subtilisin/kexin type 9
PdI	Polydispersity Index
PE	Phycoerythrin
PEG	Polyethylene glycol
Pen Strep	Penicillin/streptomycin
PI	Protease inhibitor cocktail
RIPA	Radioimmunoprecipitation assay
RISC	RNA-induced silencing complex
RNA	Ribonucleic acid
RNAi	RNA-interference

ROS	Reactive oxygen species
RPM	Rotation per minute
RT-qPCR	Reverse Transcriptase-quantitative Polymerase Chain Reaction
Rv	Reverse
siRNA	Small interfering RNA
SPT	Serine palmitoyltransferase
sWGA	Succinylated Wheat Germ Agglutinin
TBS	Tris Buffered Saline
TBS-T	Tris Buffered Saline – Tween
TE	Tris-HCl, EDTA
TNF- α	Tumour necrosis factor - α
Trypsin	Trypsin-EDTA
TX-100	Triton X-100
UMCU	University Medical Center Utrecht
VLDL	Very-low-density lipoprotein

1 INTRODUCTION

1.1 ATHEROSCLEROSIS

1.1.1 The pathology

Atherosclerosis is an immune mediated chronic inflammatory disease where plaques can build up in arteries over the whole body. Atherosclerosis is often the culprit responsible for coronary ischaemic events. On its own, atherosclerosis is hardly the cause of death. If an atherosclerotic plaque ruptures, it can cause a thrombosis. When this happens, life-threatening medical incidents can occur such as a stroke or acute coronary syndrome. (1)

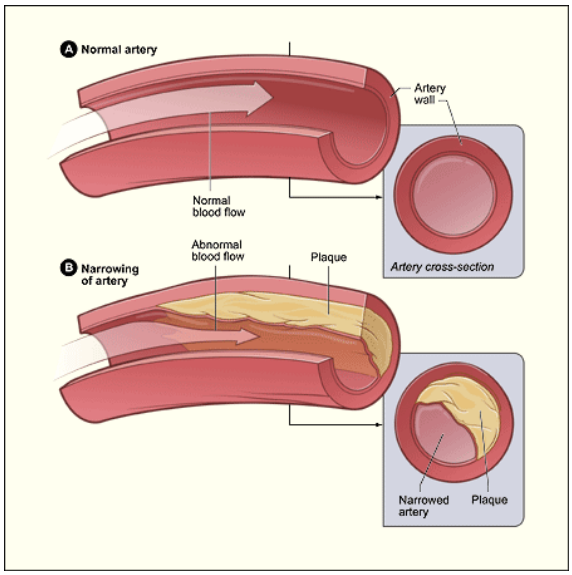

Figure 1.1: Illustration of a healthy normal artery (A) and an artery with plaque formation (B) (2)

Plaque formation, as illustrated in Figure 1.1, starts with an endothelial dysfunction caused by a disturbed laminar flow. This dysfunction makes way for low-density lipoprotein (LDL) particles to move across the endothelial layer and pile up in the intima. Being exposed to risk factors such as smoking, diabetes, hypertension et cetera allow more LDL to invade and accumulate, amplifying the endothelial dysfunction. Accumulation of LDL in the extracellular matrix ensures that the LDL particles become victims of oxidative and enzymatic alterations. The modified LDLs attract and activate different immune cells, most importantly monocytes. After the activation of monocytes, they differentiate into macrophages and express pro-inflammatory chemokines which give rise to other immune cells to invade the intima. Macrophages have the ability to phagocyte the modified LDLs and turn into foam cells. Foam cells have the capacity to release growth factors and chemokines. This can lead to inflammation and a switch of phenotype of the smooth muscle cells which causes a synthesis of extracellular components. These extracellular components add to the progress of a fibrous cap. Foam cells may also succumb to apoptosis or necrosis and discharge their lipid content in the artery wall which forms lesions. The invasion of other immune cells into the plaque coordinates reactions that might induce degradation of the plaque and lead to rupture, because of the proteases they can release. (3–5)

Plaques on their own can be asymptomatic or hinder the arterial blood flow which can lead to stabile angina. The core of a plaque is greatly thrombogenic and can be dangerous when the plaque ruptures. A rupture exposes this core to the blood and can lead to thrombosis, completely cutting off the blood flow from organs. Depending on where this rupture occurs and in what degree the blood flow is hindered, the consequences can lead up to death and disability. That is why it is important to reduce these plaques and try to prevent atherosclerosis. (1,2,6)

1.1.2 Current therapy

Since LDL are cholesterol rich lipoproteins, the current scope in treating this disease is mostly aimed at lowering the cholesterol blood concentration. A range of medicines is already on the market for this purpose. One of the most used and preferred medicines are statins, which inhibit 3-hydroxy-3-methylglutaryl-CoA (HMG-CoA) reductase in the cholesterol biosynthesis. This results in a lower total blood cholesterol level. Other cholesterol-lowering medicines such as proprotein convertase subtilisin/kexin type 9 (PCSK9) inhibitor, ezetimibe, bempedoic acid and omega-3 fatty acids can serve as alternatives if statins are not well tolerated or not working. (7,8)

Another approach is to lower the blood pressure and reduce the workload of the heart using Angiotensin Converting Enzyme (ACE) inhibitors and beta blockers. Calcium channel blockers relax blood vessels, which also lowers blood pressure. For people who suffer from angina, nitrates can be helpful to relax blood vessels. Blood sugar lowering medications such as metformin, liraglutide and empagliflozin can be used to reduce the risk factors of developing atherosclerosis.

Apart from medication, there is a big emphasis on prevention of atherosclerosis by lowering the risk factors for the disease. Eating healthy, being active, not smoking, limiting the alcohol consumption and reducing stress are a few examples of these lifestyle tips. (8)

1.2 CERAMIDE

Ceramides are formed by a condensation of palmitoyl-CoA and L-serine together with a fatty acid. It functions as a structural component in cell membranes as well as an intracellular signaller of an excess of free fatty acids. This signalling aids cells to act against the lipid load present at the time of nutritional stress for example. Ceramide can inhibit vasodilation of vascular endothelial cells and provoke cardiovascular disease this way. (9)

Atherosclerosis is a chronic inflammatory disease of the blood vessel wall. Ceramide induces the production of pro-inflammatory cytokines Interleukine-6 and C-reactive protein, resulting in increased inflammation. (10)

Moreover, reactive oxygen species (ROS) production is proved to be induced by ceramide. The mechanism behind this is the disruption of mitochondrial electron transport chain or induction of apoptosis because of modified permeability of the outer membrane of the mitochondria. ROS add to the endothelial dysfunction observed in atherosclerosis. Another component that contributes to these endothelial dysfunctions is tumour necrosis factor α (TNF- α), which accumulates in the endothelial cells. TNF-α stimulates the de novo synthesis of ceramide and activates sphingomyelinase which both result in a higher endogenous ceramide content. Sphingomyelinase converts sphingomyelin to ceramide. Ceramide in its turn can stimulate the endothelial cells to express TNF- α. This results in a vicious cycle with augmented inflammation. (9)

The infiltration of LDL in endothelial cells is one of the first steps in the plaque formation. Endogenous ceramide promotes the invasion of LDL into the endothelial cells, increasing the accumulation in the blood vessel wall. Another mechanism of ceramide in inducing plaque formation is limiting the macrophage digestion of LDL aggregates, resulting in increased foam cell formation. Ceramides could potentially play a role in the formation of atherosclerotic plaques since they are also found in high concentrations in these plaques. Several studies have shown that obstructing the de novo synthesis pathway of ceramide can lighten these lipid-induced processes. Increased plasma concentrations of ceramide are established in patients with atherosclerosis. This suggests that ceramide plasma levels are a similar diagnostic predictor as LDL plasma levels for the risk assessment of atherosclerosis. Furthermore, a causal bond between ceramide levels and atherosclerosis is established in mice studies. These findings together with all the remarks mentioned above indicate that reducing ceramide plasma levels could be a good treatment in fighting atherosclerosis. (9,10)

1.2.1 De novo ceramide synthesis

The condensation of palmitoyl-CoA and L-serine by serine palmitoyltransferase (SPT) which results in 3-keto-dehydrosphingosine, is the initial step of the de novo synthesis (Figure 1.2). 3-ketosphinganine is then reduced by 3-ketosphinganine reductase (KDSR) to sphinganine. The following step in the pathway is a catalysis by

the ceramide synthase (CerS) protein family, which adds acyl-CoA resulting in dihydroceramide with varying lengths of the acyl chain. Six different CerS proteins have been discovered in mammals. Every CerS protein has its own specificity to a substrate with a certain acyl chain length. The final step in the synthesis is the addition of a 4,5-trans double bond resulting in ceramide. The enzyme causing this conversion is dihydroceramide desaturase (DEGS). Two variants of this enzyme can be found, DEGS 1 and DEGS 2. DEGS 1 is present all over the body. DEGS 2 is mostly found in the skin, kidney and small intestine. (10)

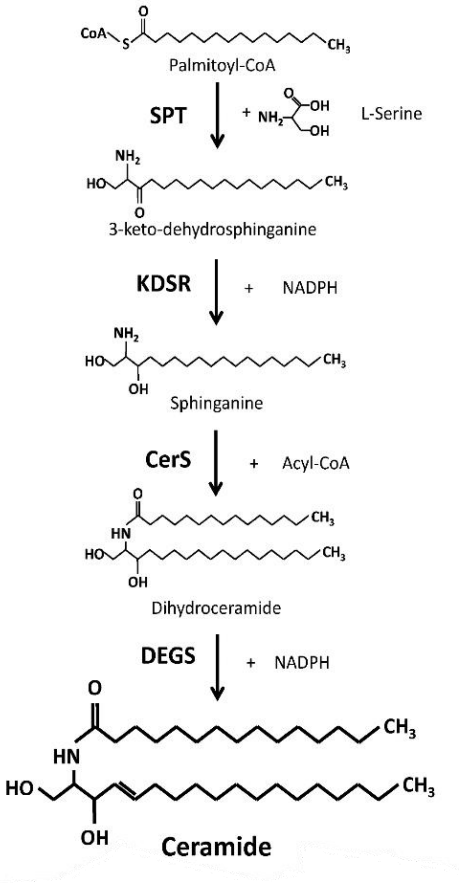

Figure 1.2: Illustration of the de novo ceramide synthesis pathway (11)

Silencing the DEGS and CerS genes could be a possible new approach for the treatment of atherosclerosis. By silencing these genes, the according enzymes can not be expressed. This results in a disturbed biosynthesis of ceramide. Especially silencing the DEGS 1 gene has shown to significantly decrease ceramide levels. The silencing of CerS has to be further explored but targeting CerS 2 showed a positive effect on reducing ceramide levels. (12,13)

1.3 NUCLEIC ACID THERAPEUTICS

Most small molecule therapies currently on the market have a short-term effect since they focus on inhibiting proteins instead of handling underlying causes of the disease. Consequently, many diseases can not be treated with small molecules. This is where nucleic acid therapeutics (NAT) have an advantage. NAT are able to have long-term effects or even cure certain diseases. They can have a gene editing, replacing, inhibiting or adding function at ribonucleic acid (RNA) or deoxyribonucleic acid (DNA) level to generate their therapeutic effects. The most important NAT on the market are antisense oligonucleotides (ASO), aptamers, gene therapy, micro RNA, small interfering RNA and ribozymes. (14,15)

1.3.1 Small interfering RNA (siRNA)

siRNA works through a mechanism called RNA-interference (RNAi). RNAi is the process of gene silencing enabled by double-stranded RNA (dsRNA) which targets

messenger RNA (mRNA), leading to degradation. When siRNA reaches the cytosol, it adheres to the RNA-induced silencing complex (RISC). In this multiprotein complex, the siRNA is cleaved by the argonaut 2 protein (Ago 2) and the sense strand is degraded. In combination with the RISC, the antisense single-strand of the siRNA forms an active RISC. The active RISC binds to mRNA with a complementary sequence to the antisense single-stranded siRNA and breaks down the bound mRNA with Ago 2. This results in a lower amount of mRNA in the cytosol of the cell, causing a decrease in expressed protein for which the mRNA encodes. (16)

Using siRNA for the DEGS and CerS gene could result in a lower expression of the two corresponding enzymes in the pathway and lead to a lower ceramide level in the body.

1.4 NUCLEIC ACID DELIVERY

The use of NAT is a very promising and attractive approach to new therapeutics as stated in section 1.3. However, the disadvantage of these therapeutics is their delivery. The negatively charged and lipophilic nucleic acids (NA) are unable to passively diffuse over cell membranes. Furthermore, NA suffer from rapid degradation by nucleases in the body and clearance by the kidney. Since NA need to arrive at the targeted tissue without modifications, they need a vehicle to be transported through the body to remain perfectly intact. (17,18)

Liposomes were the first used nanomedicine delivery vehicles. They can have one or multiple lipid bilayers with a size fluctuating between 20-100 nm. Liposomes can be used to deliver a wide range of therapeutics from small molecules to NAT. For NAT specifically, the drug carrier system should have an efficient encapsulation of the NA and be suitable for the intracellular delivery of the NA. The drawback of liposomes is the encapsulation efficiency. Neutrally charged liposomes were restricted because of very low encapsulation. This issue became less blocking with the evolution of cationic lipids. The anionic NA could interact with the cationic lipids resulting in better encapsulation. Although there was an improvement, the encapsulation still only varied between 30 and 40%. Improvements to the formation of liposomes eventually lead to the formation of lipid nanoparticles. Because of the ionizable group on the cationic lipid, the NA are stabilized after complexation resulting in high encapsulation efficiencies. (17,18)

1.5 LIPID NANOPARTICLES (LNPs)

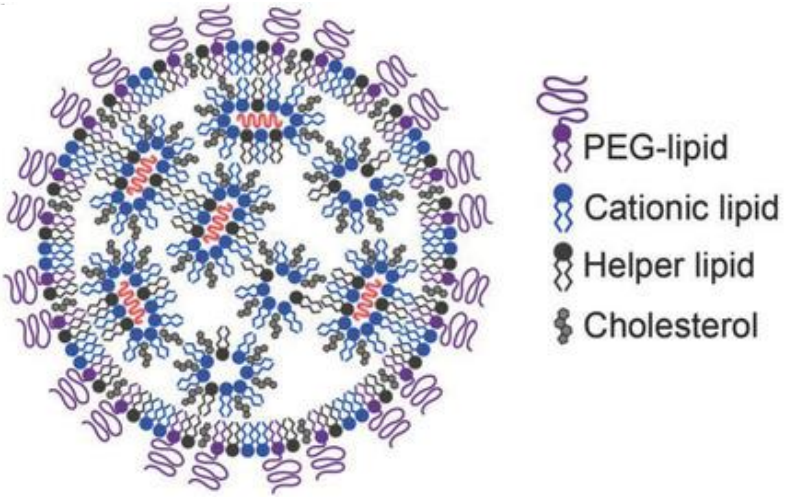

Figure 1.3: Illustration of the proposed structure of a lipid nanoparticle with inverted micellar structures encapsulating the siRNA (red). (18)

LNPs can be defined as spherical lipid vesicles and are used as non-viral carriers for NAT delivery (Figure 1.3). The first LNP encapsulated with siRNA that came onto the market was patisiran (Onpattro®), which is used for transthyretin-induced amyloidosis. This LNP consists of 4-(dimethylamino)-butanoic acid, (10Z,13Z)-1-(9Z,12Z)-9,12-octadecadien-1-yl-10,13-nonadecadien-1-yl ester (DLin-MC3-DMA) as an ionizable amino lipid, 1,2-dimyristoyl-rac-glycero-3-methoxypolyethylene glycol-2000 (DMG-PEG2000) as a PEG-lipid, cholesterol and helper lipid 1,2-Distearoyl-sn-glycero-3-phosphocholine (DSPC). Most of the current LNPs are based on this formulation. (19)

1.5.1 Ionizable amino lipid

One of the most important components of an LNP is the ionizable amino lipid. This lipid has a headgroup with positive charge, a hydrophobic tail and a linker to connect the 2 previous groups. The pKa of the headgroup is about 6.5, so the lipid is neutral at physiological pH (pH 7.4) and positively charged at acidic pH. One of the purposes of the lipid is the entrapment of a nucleic acid at a low pH. The positive charge of the headgroup interacts with the negatively charged phosphate groups on nucleic acids, resulting in a high encapsulation efficiency of the NA. The pH is increased to physiological pH after the LNP formation, turning the ionizable lipid neutral again.

The main pathway for LNPs to get taken up is via endocytosis. This route consists of endosomes, which are vesicles with an internal pH of 5. The endosomes mature from early to late endosomes. Late endosomes fuse with lysosomes which contain digestive enzymes. If the LNPs do not escape from the endosome in time, they will be

degraded in the lysosomes. Ionizable lipids aid the endosomal escape of the LNP cargo into the cell. Because of the low pH in the endosome, the ionizable lipid has a positive charge. This is optimal to interact with the anionic lipid bilayer of the endosome. Ionizable amino lipids can bind to the lipid bilayer of the endosome and cause stress or tension on the membrane. If the tension is strong enough, pores are created in the membrane. The cargo of the LNP can be released into the cytosol of the cell through these pores and the nucleic acid can perform its function (Figure 1.4). (20)

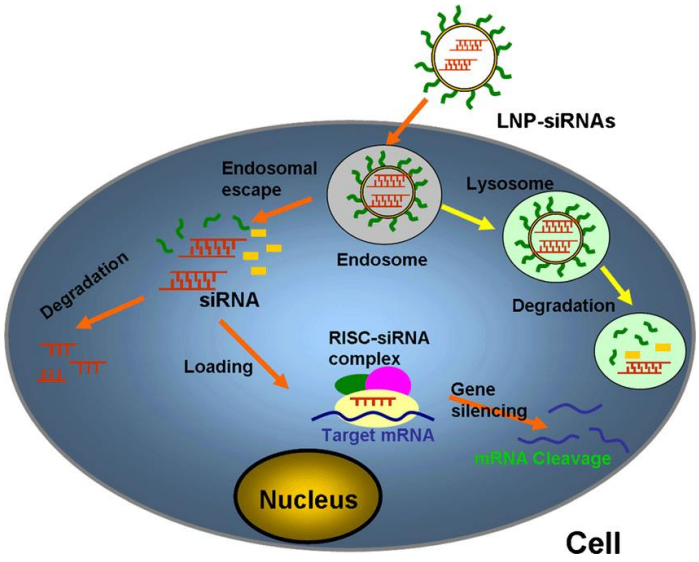

Figure 1.4: Illustration of endosomal uptake of LNPs with cargo release and siRNA induced RNAi leading to cleavage of mRNA. (21)

1.5.2 Polyethylene glycol-lipid

Polyethylene glycol (PEG) is an important component of an LNP. It forms a hydrophilic layer to cover the surface of the LNP. The interaction between lipoproteins and plasma proteins (e.g. complement components) in the circulation after administration is decreased because of the hydrophilic environment. This way the lipid protects the LNP against opsonisation and uptake by phagocytes, which prolongs the circulation time of the LNP. Another advantage is the prevention of aggregation of LNPs, resulting in more stable LNPs. However, the PEG percentage in an LNP should be limited. A higher PEG ratio makes it harder for the LNP to interact with the membrane of the cells and induce endocytosis. Contact with the endosomal membrane is required for endosomal escape. PEG interferes with this interaction and obstructs endosomal escape. In other words, PEG is necessary for the stability and a prolonged half-life of LNPs, but an excess of PEG counteracts the endosomal escape. This phenomenon is also known as the “PEG dilemma”. (22)

1.5.3 Cholesterol

Cholesterol is naturally a part of the eucaryotic cell membrane. It has a condensing effect on acyl chains, which is called the “condensation effect”. Because of this effect, the lipid packaging in the LNPs is tighter, which lowers the permeability. It has been stated that cholesterol has the ability to transfer between lipid bilayers, resulting in an equilibration of a concentration gradient. This means that addition of cholesterol in the LNP helps to protect the particle stability. (18,23)

1.5.4 Helper lipid

DSPC is one of the most used helper lipids for siRNA-LNPs. It assists the bilayer formation and balances the LNP. The structure of the lipid consists of two acyl chains with a polar headgroup, which forms a cylindrical geometry. Through computer modelling, it was found that DSPC possibly interacts with siRNA. This suggests that it has a roll in the encapsulation of siRNA. (18)

1.5.5 LNP formation

The principle of the LNP formation is based on self-assembly of the lipids. The first step is the interaction between the negatively charged NA and the positively charged cationic lipid caused by a spontaneous reaction via electrostatic interactions. Afterwards, the LNP develops by van Der Waals and lipophilic interactions among the lipid components. The lipid phase containing all the lipids and the aqueous phase containing the NA are rapidly mixed, resulting in lipid nanoparticles by microfluidic hydrodynamic focusing (MHF). The principle of this technique is the precipitation of the lipid components by diluting them in the aqueous phase, leading to a more hydrophilic environment. The change in polarity makes it more energetically favourable for the lipids to come together and form spherical vesicles (Figure 1.5). (18)

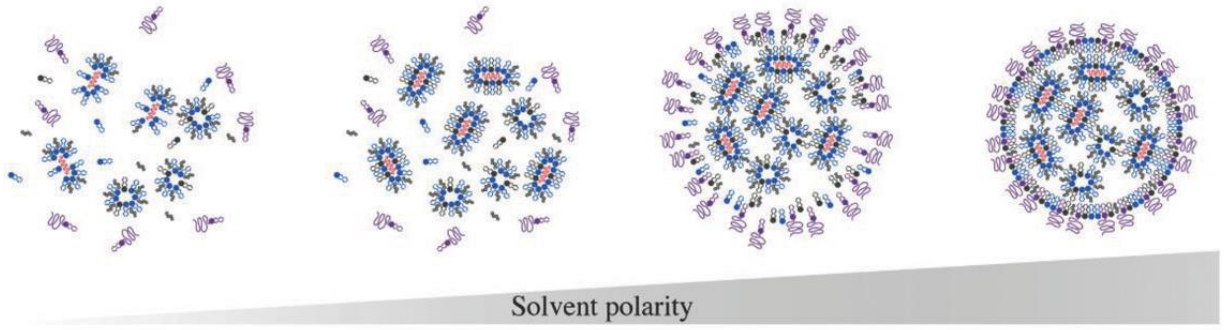

Figure 1.5: The formation of LNPs with increasing polarity. The first step is the interaction between the siRNA and cationic ionizable lipid. The self-assembly of the lipids is driven by the increase of polarity in the solvent. (18)

1.5.6 Nitrogen-to-phosphate (N/P) ratio

The N/P ratio is the ratio of the cationic charge of the amino group of the ionizable lipid and the anionic charge of the phosphate group of the nucleic acid backbone. This ratio is of big importance for the formulation of LNPs since this ratio lies at the basis of the first step of the LNP formation. Increases in the ratio can lead to improved therapeutic effects. This indicates that the ionizable lipids that do not combine with NA, are available to improve endosomal escape. (18)

1.5.7 Size

The diameter of the LNP plays a crucial role in the pharmacokinetics of the LNP. Smaller particles experience less clearance from the circulation resulting in a longer half-life. A size under 100 nm is favoured for hepatocyte targeting since the particles can easily pass through the liver fenestrae. The stability of the LNPs is also affected by the size. The ionizable lipid is less easily detached from the LNP in larger particles, leading to a higher efficiency. In conclusion, the LNP-uptake and therapeutic effect are driven by the size. (18)

1.6 LIVER TARGETING

The liver does not have a basal lamina as a barrier in contrary to the majority of tissues. This characteristic together with good circulation leads to a rapid build up of LNPs in the liver after systemic administration. This passive route is mostly regulated by the size and charge of the particles. Modifying the lipid phase composition can change the size and charge of LNPs and increase uptake. Raising the PEG-ratio can alter the size and using cholesteryl hemisuccinate for example gives a negative charge to the LNP, which favours the liver. Furthermore, including an additional lipid to the lipid phase can be used to realize this passive targeting. (24,25)

Even though passive targeting by adjusting physicochemical properties of LNPs is enough to target the liver, it is not sufficiently specific for the targeting of particular cell types, such as hepatocytes. To actively target cells, a ligand for a specific receptor on the cell surface can be inserted onto the surface of the LNP. Passive targeting can occur first so LNPs start to accumulate in the liver tissue, after which the specific ligand interacts with its receptor. The specific ligand-receptor binding results in endocytosis. Even though most of the LNPs accumulate in the liver, active targeting is still relevant since the liver has hepatocytes, hepatic stellate cells, Kupffer cells and sinusoidal endothelial cells. Hepatocytes are the most important for the synthesis of ceramide.

This makes targeting the hepatocytes the most ideal approach for silencing genes in the ceramide synthesis. (26)

1.6.1 Endogenous targeting

Upon injection of LNPs into the bloodstream, serum proteins can interact with the particles and form a protein-coated interface (also called “protein corona”) by transferring components. One of these proteins is apolipoprotein E (Apo E), which is naturally present in the body. It has been investigated that after addition to the LNPs, Apo E adsorbs onto the LNP surface and even rearranges itself into the lipid core of the particle. (27)

Apo E serves as a part of lipoproteins, which are involved in the transportation of lipids between organs or inside specific tissues. It is mostly linked to chylomicron remnants, high-density lipoproteins (HDL) and very-low-density lipoproteins (VLDL). The clearance of these lipoproteins is controlled by Apo E by binding to the low-density lipoprotein receptor (LDLR). This specific ligand-receptor interaction leads to a LDLR-mediated endogenous targeting of hepatocytes. (28,29)

LDLR is a transmembrane glycoprotein present on the cell membrane. It exerts its effect by the binding and internalization of lipoproteins composed of cholesterol in the blood. The receptor has a high expression all over the body but especially on hepatocytes since it is an important part of the cholesterol regulation in the body. Not only LDL but also HDL, chylomicron remnants and VLDL can be recognised by the receptor and taken up via receptor-mediated endocytosis. While the particles get lysed in the lysosome, the receptors are recycled back to the membrane of the cell. (30)

Apo E conjugated LNPs have already been shown to increase the hepatic uptake and silencing effect of siRNA-LNPs. But further investigation is still needed before translation to in vivo mice studies.

1.6.2 Exogenous targeting

N-acetyl-galactosamine (GalNAc) is a sugar molecule that binds specifically to the asialoglycoprotein receptor (ASGPR) which has a high expression on hepatocytes. The receptor has a function in the regulation of glycosylated serum protein homeostasis. It has a specific recognition for carbohydrates with a high affinity for GalNAc. ASGPR is a transmembrane protein that consists of two subunits, ASGPR 1

and ASGPR 2. ASGPR 1 is the most important subunit regarding GalNAc-mediated uptake of LNPs. The ASGPR 2 subunit has no significant role for the uptake. (29,31)

The ASGPR was found to have a flat binding pocket, which enables the receptor to bind multiple GalNAc groups at the same time. For this reason, tri-GalNAc has a higher affinity for the receptor than the monovalent form. Binding of GalNAc to the receptor initiates endocytosis, followed by lysosomal degradation and receptor recycling to the cell membrane. Since clustered GalNAc does not naturally occur in the body, it is seen as an exogenous ligand for the receptor. (32)

GalNAc conjugation to NAT has been proved to work. GIVLAARI™ is one of the examples that is already approved and available on the market. It is an siRNA conjugated with GalNAc. Even though the GalNAc conjugation to siRNA has already been well investigated, little investigation around conjugation of GalNAc on LNPs has been conducted. (33)

2 OBJECTIFS

The primary aim of this project is to investigate the in vitro liver targeting by using two different approaches: Apo E and GalNAc. These are both ligands for two different highly expressed receptors on the liver, LDLR and ASGPR 1. By incorporating GalNAc or Apo E in the LNPs, they form liver-targeted LNPs.

The practical method for this project was to first develop targeted LNPs with enhanced green fluorescent protein (eGFP) mRNA labelled with Cyanine 5 (Cy 5) to verify if the targeting leads to a better uptake and transfection of the mRNA. The LNPs were transfected in a hepatocarcinoma cell line, HepG2, as an in vitro substitute for hepatocytes and human embryonal kidney cells (HEK293FT) as a control cell line. Since Cy 5 labelled eGFP mRNA is fluorescently detectable, the signal of the transfected cells could be measured using flow cytometry.

Once the effectiveness of the targeting was established, targeted LNPs were developed with androgen receptor siRNA to prove that the targeting was also noticeable on gene silencing level. The silencing effect was measured with western blot as well as Reverse Transcriptase-quantitative Polymerase Chain Reaction to verify silencing on protein and mRNA level, respectively.

The LNPs were characterised to gather information about the size of the particles, the size distribution and the percentage of encapsulated RNA. A RiboGreen assay was used to determine the encapsulation efficiency and the concentration of RNA in the LNPs. Dynamic light scattering was applied to define the size and polydispersity index of the LNPs. The LNPs with GalNAc were additionally characterised to verify if GalNAc was present on the LNP surface with a dot blot. For this dot blot, fluorescein labelled lectins were used to specifically bind to GalNAc instead of antibodies, which are conventionally used in these kinds of assays.

An additional assay was performed to check the expression of ASGPR 1 on both cell lines. This was done with a surface coating assay with Phycoerythrin (PE)-labelled antibodies which could be analysed using flow cytometry.

3 MATERIALS AND METHODS

3.1 LNP FORMULATION

3.1.1 Materials

DLin-MC3-DMA was ordered from Med chem express (Monmouth Junction, New Jersey, USA). Cholesterol was ordered from Sigma Aldrich (Steinheim, Germany). DSPC was ordered from Lipoid GmbH (Ludwigshafen, Germany) and DMG-PEG2000 was ordered from Avanti Polar Lipids Inc. (Alabaster, Alabama, USA).

1,2-distearoyl-sn-glycero-3-phosphoethanolamine-N-[tris-GalNAc-GABA-(polyethylene glycol)-2000] (GalNAc-PEG) was ordered from Sussex Research (Ontario, Canada). Recombinant human Apolipoprotein E3 (Apo E) was ordered from Abcam Inc (Cambridge, UK). eGFP mRNA labelled with Cy 5 was made in the Central Diagnostic Laboratory (CDL) department of the University Medical Center Utrecht (UMCU)(Utrecht, the Netherlands). Androgen receptor (AR) siRNA was ordered from Integrated DNA Technologies (Leuven, Belgium).

3.1.2 Non-Targeted (NT) LNP formulation

To prepare the lipid phase, DLin-MC3-DMA, cholesterol, DSPC and DMG-PEG2000 were dissolved in absolute ethanol (Merck, Darmstadt, Germany) to obtain a molar ratio of 50:38,5:10:1,5 (DLin-MC3-DMA:cholesterol:DSPC:DMG-PEG2000). A formulation buffer was prepared by making a 100 mM sodium acetate solution and adjusting the pH with acetic acid to pH 4. The aqueous phase was prepared by adding the calculated amount of Cy 5-eGFP mRNA or AR siRNA to the formulation buffer. For the mRNA LNPs a N/P ratio of 5 was used and for the siRNA LNPs a N/P ratio of 6.

Before formulating the LNPs, the NanoAssembler cartridge was primed with formulation buffer and absolute ethanol. The priming was done with a flow ratio of 1:1 (aqueous:ethanol) in the NanoAssembler (Precision Nanosystems, Vancouver, Canada). After the priming, the aqueous and lipid phase were filled in separate syringes and loaded onto the cartridge. The settings for the formulation were changed to a flow ratio of 3:1 (aqueous:lipid). The formed LNPs were collected in a 15 mL tube. In between runs, the cartridge was flushed with absolute ethanol and formulation buffer using the same settings as the priming. After the final run, the cartridge was also flushed with air. The complete settings for the NanoAssembler are given in Table 8.1.

A 20 kDa (kilo Dalton) Slide-A-Lyzer cassette (ThermoFisher scientific, Rockford, Illinois, USA), was hydrated for 2 min in Phosphate Buffered Saline (PBS)(House made, CDL UMCU, Utrecht, The Netherlands) before loading the LNPs in the cassette. The formulated LNPs were taken up with a needle and syringe and transferred to the cassette. The cassettes were put in 4 L of PBS overnight in a cold room at 4°C to remove the ethanol and unencapsulated RNA and increase the pH to 7. After the overnight dialysis, the LNPs were taken out of the cassette and transferred to an Eppendorf. A part of the LNPs were stored at 4°C for short term use. The other part was stored in the freezer at –20°C in 8% (V/V) sucrose for long term use.

3.1.3 In situ GalNAc LNP formulation

The in situ GalNAc LNPs were prepared in the same way as the NT LNP explained in 3.1.2. The difference with the NT LNP is the composition of the lipid phase. A fraction of the DMG-PEG2000 was substituted with the GalNAc-PEG. For example to prepare the LNPs with a molar ratio of 0.25% GalNAc, a molar ratio of 0.25% GalNAc-PEG and 1.25% of DMG-PEG2000 was added. This way, the combination of GalNAc-PEG and DMG-PEG2000 remained 1.5% so the ratios of the other components of lipid phase stayed the same. LNPs with a molar ratio of 0.25%, 0.5% and 1% GalNAc were prepared for mRNA LNP formulations. For siRNA LNP formulations, only 0.25% GalNAc was prepared.

3.1.4 Post-insertion GalNAc LNPs

For the post-insertion of GalNAc on the NT LNP, the volume of GalNAc-PEG to add was calculated based on the desired molar ratio of GalNAc and the volume of the LNPs. LNPs with a molar ratio of 0.05%, 0.15% and 0.25% were prepared for mRNA LNP formulations. The calculated volume of GalNAc-PEG was pipetted in an Eppendorf with 1 mL of the NT LNP. The mixture was vortexed and incubated in a warm water bath at 40°C for 2 h, protected from light. After the incubation period, the LNPs were transferred to a 20 kDa cassette and put in a bucket with 4 L PBS. The bucket was placed in a cold room at 4°C overnight to dialyse and remove unbound GalNAc-PEG.

3.1.5 Post-insertion Apo E LNPs

Apo E was post inserted on the NT LNP right before transfecting the cells with them. A 49:1 (lipid concentration:Apo E) weight ratio was used to coat the LNPs. Apo E was added to the LNPs in an Eppendorf and incubated for 10 min at 37°C. (34)

3.2 LNP CHARACTERISATION

3.2.1 Dynamic light scattering (DLS) and Polydispersity Index (PdI)

3.2.1.1 Principal

Dynamic light scattering is used to measure the Brownian motion of macromolecules, which can be correlated to the size of particles. The random movement of particles caused by collision of solvent molecules in solution is defined by the Brownian motion. The bigger the particles, the lower the Brownian motion will be since larger particles move slower. This motion can be measured by monitoring the movement of particles over different time points. The smaller the particles are, the faster they move. This way they will not be detected in the same position over time, in contrast to larger particles.

Light will scatter in different directions when a laser light is send through a solution containing macromolecules, such as LNPs. The scattering intensity of the light can be recorded by a detector in a DLS instrument. The PdI is calculated from the broadness of the size distribution that is measured. (35-37)

3.2.1.2 Method

Dynamic light scattering was detected with a ZetaSizer Nano S (Malvern Panalytical, Malvern, UK). The samples were prepared by diluting the LNPs 1:20 in Dulbecco's Phosphate Buffered Saline (DPBS) (Sigma Aldrich, Steinheim, Germany). 30 µL of LNP sample and 570 µL of DPBS were transferred to a cuvette. The size and PdI were measured three times with 13 runs per measurement. The mean of these three measurements was calculated.

3.2.2 RiboGreen assay

3.2.2.1 Principal

To define the encapsulation efficiency of the RNA in the LNPs and the encapsulated RNA concentration, a RiboGreen assay was used. A calibration curve was made to compare the samples with and to be able to calculate the concentration of RNA in the samples. The LNP samples were diluted to have a concentration that falls within the concentrations of the calibration curve. The encapsulation efficiency can be determined by comparing the unencapsulated RNA outside of the LNPs and the RNA amount inside the LNPs. The samples and calibration curve were both analysed in Tris-HCl, ethylenediaminetetraacetic acid (EDTA) (TE)-buffer and 2% Triton X-100 (TX-100). The LNPs were analysed in a TE-buffer to estimate the unencapsulated

RNA. TX-100 is a detergent that lyses the LNPs so the RNA inside the LNPs is released. The samples analysed in Triton X-100 were used to determine the total RNA concentration which is the concentration in and outside of the LNP. The Quant-iT™ RiboGreen™ RNA reagent is a green fluorescent dye that emits fluorescence upon binding RNA. The reagent excites light at 485 nm and emits at 530 nm. (38)

3.2.2.2 Method

For this assay, a Quant-iT™ RiboGreen® RNA Assay Kit (Invitrogen, Eugene, Oregon, USA) was used. First, the 20x TE stock solution of the kit was diluted to a 1x TE-buffer with Nuclease free water (Integrated DNA Technologies, Leuven, Belgium). A 2% (V/V) TX-100 was prepared by adding 200 µL of TX-100 (BDH, Dubai, UAE) to 10 mL TE buffer. An RNA stock solution of 20 µg/mL was prepared from the 100 µg/mL RNA stock solution of the kit by diluting 30 µL RNA stock with 120 µL TE-buffer. Out of the 20 µg/mL stock solution, a calibration curve was prepared according to Table 3.1.

Table 3.1: Volumes to prepare the calibration curve

Concentration (µg/mL)[a]	Volume stock solution (µL)[b]	Volume TE-buffer (µL)
4	50	200
3	37.5	212.5
2	25	225
1	25	475
0.5	200 (1 µg/mL)[c]	200
0.25	200 (0.5 µg/mL)[d]	200
0	0	200

[a] The final concentration of the calibration curve samples obtained after adding the volumes of stock solution and TE together

[b] Volumes of the 20 µg/mL stock solution

[c] The volume of 1 µg/mL sample to add

[d] The volume of 0.5 µg/mL sample to add

The samples analysed in TE-buffer, were diluted 5 times. The 1:5 dilution was obtained by diluting 14 µL of LNPs with 56 µL TE-buffer. The samples for the TX-100 wells, were diluted 50 times by taking 6 µL of the 1:5 dilution and adding it to 54 µL TE-buffer.

25 µL of the calibration curve was added in quadruple to a flat-bottom black 96-well plate (Greiner Bio-one, Frickenhausen, Germany). 25 µL of the LNP sample dilutions were added in duplicate. 25 µL of TE-buffer was added to 2 of the calibration curves and to the 1:5 samples. 2% TX-100 was added to the remaining 2 calibration

curves and to the 1:50 samples. Afterwards, the plate was incubated for 5-10 min at 600 rotations per minute (RPM) on a plate shaker. Meanwhile the RiboGreen solution was prepared by diluting the Quant-iT™ RiboGreen™ RNA reagent 200x with TE-buffer. 50 µL of the RiboGreen solution was added to each well. The plate was covered with aluminium foil and incubated for 5 min on a plate shaker at 300 RPM. The fluorescence of the samples was measured at excitation of 485 nm and emission of 530 nm with a SpectraMax iD3 (Molecular Devices, San Jose, California USA).

To determine the encapsulation efficiency, the concentration of the TE samples and TX-100 samples were calculated using standard addition with the calibration curve. By dividing the TE concentration by the TX-100 concentration and multiplying it by 100%, the unencapsulated RNA percentage was obtained. The encapsulation efficiency was determined by subtracting 100% by the unencapsulated percentage. The concentration of encapsulated RNA was obtained by subtracting the TX-100 RNA concentration by the TE RNA concentration.

3.2.3 Dot blot

3.2.3.1 Principal

Spotted samples get fixed on the membrane by drying. When the lectin is added to the membrane, it binds specifically to the sugar groups present on the membrane. After this incubation the unbound lectin is washed away to reduce the background signal. The used lectin is fluorescein labelled, which makes it easily detectable by measuring the fluorescence. To avoid nonspecific binding of the lectin, the membrane was blocked prior to the lectin incubation. This way, all the “non-used” spots on the membrane are occupied by a nonspecific protein. (39)

3.2.3.2 Method

A piece of nitrocellulose membrane was cut off and marked with a pencil to indicate where the spot was going to be. The GalNAc-PEG stock was 1:4 diluted with DPBS as a positive control. 2 µL of each sample, the positive control and DPBS as negative control were spotted under the indicated place on the membrane. The membrane was air dried for a few minutes before adding the buffer. The non-specific sites were blocked by wetting the membrane in Intercept® Blocking Buffer (LI-COR® Biosciences, Lincoln, Nebraska, USA):Tris Buffered Saline (TBS)(House made, CDL UMCU, Utrecht, The Netherlands) (1:1) for 1 h at room temperature. Afterwards, the membrane was incubated with 5 µg/mL succinylated Wheat Germ Agglutinin (sWGA)(Vector Laboratories, Newark, California, USA). The lectin was diluted with

Blocking Buffer: Tris Buffered Saline – Tween (TBS-T)(House made, CDL UMCU, Utrecht, The Netherlands) (1:1). TBS-T contains 0.1% Tween. After a 2 h incubation of the membrane with sWGA, the membrane was washed three times with TBS-T and one time with TBS for 5 min. The fluorescence of the spots on the membrane was measured by an Odyssey® M (LI-COR® Biosciences, Lincoln, Nebraska, USA) on a 488 nm channel. (40,41)

3.3 CELL CULTURE

3.3.1 Materials

For the experiments, HEK293FT and HepG2 cell lines were used. The HepG2 cells were provided by Anil Kumar Deshantri (CDL UMCU, Utrecht, The Netherlands) and the HEK293FT cells by Songpu Xie (CDL UMCU, Utrecht, The Netherlands). HepG2 is a hepatocarcinoma cell line that highly expresses the ASGPR 1 and LDLR. For this reason, this cell line is used to investigate the hepatic targeting. HEK293FT is a fast growing human embryonal kidney (HEK) cell line which has a low expression of the LDLR and no expression of ASGPR 1. For this reason, the HEK cells are used as a negative control cell line. Both cell lines were cultured at 37°C and 5% CO_2 in Dulbecco's Modified Eagle Medium (DMEM) with addition of 10% fetal calf serum (FCS) and 1% penicillin/streptomycin (Pen Strep), called DMEM +/+ hereafter. DMEM, Opti-MEM®, 0.5% Trypsin-EDTA (10x)(Trypsin) and Pen Strep were ordered from Gibco (Waltham, Massachusetts, USA). FCS was ordered from Cytiva (Marlborough, Massachusetts, USA). The cells were cultured in T75 cell culture flasks, which have a surface of 75cm^2.

3.3.2 Passaging cell lines

Before passaging, the cells were checked under a microscope to estimate the confluence. The medium was aspirated from the flask and the cells are washed with 10 mL DPBS. 10x Trypsin was first diluted to 1x Trypsin with DPBS. 3 mL Trypsin was added to the cells and the flask was incubated for 5 min at 37°C. When the cells were detached, warm DMEM +/+ was added to the flask according to the wanted dilution. The cells were resuspended in the medium by pipetting up and down. Thereafter the calculated volume of cells was transferred to a new flask, based on the desired passaging factor. Warm DMEM +/+ was added to the new flask to obtain a total volume of 15 mL. The cells were hereafter incubated at 37°C and 5% CO_2.

3.3.3 Freezing cell lines

Cells can be frozen at –80°C to store for later use. To freeze cells, they need to be counted, to be sure how many cells are frozen per vial. Cells should be stored in DMEM+/+ with 10% (V/V) dimethyl sulfoxide (DMSO)(Merck, Darmstadt, Germany). To prepare this solution, 5 mL of sterile filtered DMSO was added to 45 mL DMEM +/+.

The medium from the flask was aspirated and the cells were washed with 10 mL DPBS. 3 mL Trypsin was added to the cells and the flask was incubated for 5 min at 37°C. 9 mL DMEM+/+ was added to the cells to deactivate the Trypsin. The cells were transferred to a 50 mL tube and centrifuged for 5 min at 300 RPM. After aspirating the medium, a pellet of cells was left in the tube. The volume of DMEM+/+ 10% DMSO to obtain 5 million cells/mL was calculated and added to the cells. The cells were well resuspended by pipetting them up and down in the medium. 1 mL of the cell suspension was pipetted into a Nunc™ CryoTube™ Vial (Thermo Fischer scientific, Jiangsu, China). All the vials were placed in a CoolCell LX (Biocision, Waltham, Massachusetts, USA) and stored at -80°C.

3.4 TRANSFECTION ASSAY

3.4.1 Cell counting

First, the medium from the flask was removed. The cells were washed with DPBS and 3 mL Trypsin was added to the cells. After a 5 min incubation at 37°C, the cells were resuspended in warm DMEM +/+ and transferred to a 15 mL tube.

10 µL of cell suspension was transferred to an Eppendorf together with 10 µL of Trypan Blue solution (Sigma-Aldrich, Steinheim, Germany). The cells were resuspended in the Eppendorf and 10 µL of the suspension was pipetted onto the counting chamber. The counting chamber and coverslip were cleaned with 70% ethanol and airdried prior to using it. The counting chamber was inserted into the Luna II Automated Cell Counter (Logos Biosystems, Villeneuve d'Ascq, France). The cells were counted with a 1:2 dilution and Trypan Blue protocol. The live cell count was written down and used for further calculations. After counting the cells, the counting chamber was first cleaned with demineralised water (demiwater) and afterwards with 70% ethanol.

3.4.2 Gelatine coating 96-well plate

The HEK293FT cells tend to detach easily. For this reason, the 96-well plate for this cell line is coated with gelatine beforehand. (42) 50 µL 0.1% gelatine solution was pipetted in every well to seed. The gelatine solution was made from Bovine skin gelatine (Sigma Aldrich, Steinheim, Germany). The 96-well plate was incubated with the gelatine for at least 1 h at 37°C. After the incubation, the gelatine solution was aspirated and 100 µL DMEM +/+ was added to every well. After another hour of incubation, the medium was removed off the plate right before seeding the cells onto it. (43)

3.4.3 Seeding

The purpose of the seeding is to seed 24000 cells/well for HEK293FT and 50000 cells/well for HepG2 for the fluorescence activated cell sorting (FACS) analysis. For the western blot and Reverse Transcriptase-quantitative Polymerase Chain Reaction (RT-qPCR) analysis, 16000 cells/well and 40000 cells/well were seeded for HEK293FT and HepG2 respectively. Prior to seeding, the cells were counted as explained in section 3.4.1. The volume of cell suspension and medium to add to a 15 mL tube were calculated based on the live cell count and volume to seed per well with an excess of 1.3. After adding the calculated volume of cell suspension and DMEM +/+, the cells were resuspended well.

A multichannel pipette was used to pipette 150 µL of cell suspension/well into a tissue culture treated flat-bottom 96-well plate with lid (Corning incorporated, Kennebunk, Maine, USA). 150 µL of DPBS was added to the border wells of the plate to prevent the cells from drying out. After the seeding, the plate was incubated at 37°C.

3.4.4 Transfection protocol

3.4.4.1 LNP dilutions

The LNPs were diluted using Opti-MEM® to obtain a dose of 200 ng RNA/well. The calculations were based on the concentrations of encapsulated RNA of the LNPs with an excess of 1.2.

3.4.4.2 Protocol 1

The seeded cells were washed with 150 µL Opti-MEM® after the medium from the wells on the plate was aspirated with a multichannel pipette. 160 µL of Opti-MEM® + 1% Pen Strep and 40 µL of the LNP dilutions or 40 µL DPBS for the negative control were added in triplicates to the cells. The cells were incubated for 6 h with the LNPs

after the transfection. After 6 h, the medium was aspirated from the cells and 200 µL Opti-MEM® + 1% Pen Strep was added. The cells were incubated for 30 min with Opti-MEM® + 1% Pen Strep to wash. The medium was removed after the 30 min incubation and 200 µL of Opti-MEM® + 1% Pen Strep was added to the cells. The cells were then incubated overnight at 37°C.

3.4.4.3 Protocol 2

The medium from the seeded cells on the plate was aspirated with a multichannel pipette. 160 µL of Opti-MEM® + 1% Pen Strep and 40 µL of the LNP dilutions or 40 µL DPBS for the negative control were added in triplicates to the cells. After the transfection, the cells were incubated for 6 h with the LNPs. The medium was aspirated from the cells and 200 µL DMEM+/+ was added after the incubation. The cells were incubated overnight at 37°C for FACS analysis and 48 hours for western blot and RT-qPCR analysis.

3.4.5 FACS analysis

3.4.5.1 Principal

FACS is a type of flow cytometry which detects single cells while passing through multiple lasers. The scatter of visible light can be measured in two different ways: forward and side scatter. Forward scatter is measured in the forward direction. It gives an indication of the cell size. The longer the laser is interrupted, the bigger the cell. Side scatter is measured at a 90° angle and indicates the granularity or internal structure of the cells. Apart from sorting the cells by size, the lasers can excite fluorochromes on the cells, which emit fluorescence. This fluorescence can be measured in different channels. (44,45)

The Cy 5 label falls within the allophycocyanin (APC)-channel, which has an excitation maximum at 652 nm and emits at 658 nm. The signal of the eGFP protein can be detected in the fluorescein isothiocyanate (FITC)-channel. This channel has an excitation peak at 491 nm and an emission peak at 516 nm. Since these two channels do not overlap, both can be measured at the same time. Cy 5 gives an indication of the cell population that takes up the LNPs. If the LNP gets taken up, the Cy 5 label is present in the cell and gives a detectable fluorescent signal. If the mRNA gets transfected in the cells, they start to express the eGFP protein, which is fluorescently detectable. (46,47)

3.4.5.2 Method

Cells were seeded and transfected with mRNA LNPs as mentioned in sections 3.4.3 and 3.4.4.3. The medium was aspirated of the transfected cells using a multichannel pipette and 200 µL DPBS was added to the wells to wash the cells. After aspiration of the DPBS with a multichannel pipette, 50 µL Trypsin was added to the cells. 200 µL DPBS 2% FCS was added to the wells after a 5 min incubation at 37°C with the Trypsin. DPBS 2% FCS was prepared by adding 1 mL FCS to 49 mL DPBS in a 50 mL tube. After resuspending the cells by pipetting up and down, 240 µL of the cell suspension was transferred to a flat-bottom 96-well FACS plate. The samples were analysed using a BD FACSCanto™ II (BD Biosciences, Franklin Lakes, New Jersey, USA).

The gatings were set to only include the single cells. The mean of the APC-Area signals and of the FITC-Area signals were divided by the mean signal of the NT LNP sample to normalise for the differences between the different experiments. The mean of the normalised values from the different experiments was plotted. To calculate if the results are statistically significant a two-way Analysis of variance (ANOVA) test with multiple comparisons was used.

3.4.6 Western blot analysis

3.4.6.1 Principal

Western blot has the same principal as a dot blot which is already mentioned in section 3.2.3.1. However, they differ in that the samples are first separated by gel electrophoresis and then blotted onto a membrane by an electrical field. The proteins get separated in the gel by size. Since the pores in the gel get smaller on the lower part of the gel, smaller proteins move faster through the gel resulting in lower bands. The nonspecific spots are first blocked before adding a specific antibody to the membrane. Since the primary antibody is not fluorescently labelled, a secondary antibody with fluorescent label is added to the membrane to bind the primary antibody and make it detectable. (48)

In one of the repetitions of this assay a reversible protease inhibitor, MG-132, was added to the cells. The purpose of this inhibitor was to counter the protease function of the cell, resulting in a decreased protein breakdown. This way the protein concentration in the cell should be higher when lysing them.

3.4.6.2 Method

After seeding and transfecting the cells with siRNA LNPs as mentioned in sections 3.4.3 and 3.4.4.3, the cells were prepared as samples for western blot 48 h post-transfection by using radioimmunoprecipitation assay-buffer (RIPA)(VWR international, Radnor, Pennsylvania, USA) + protease inhibitor cocktail (PI)(1:100) (Sigma-Aldrich, Steinheim, Germany) to lyse them for the first assay.

The procedure was repeated with the adaptation of adding 1 µM MG-132 to the cells 16 h prior to lysing them. A stock solution of 30 mg/mL MG-132 (Sanbio B.V., Uden, The Netherlands) in DMSO was diluted 1:315 to 200 µM. 1 µL of 200 µM MG-132 was added to the cells to obtain a total concentration of 1 µM in 200 µL.

Since 3 wells were transfected per condition, 1 sample was made out of these 3 wells. The medium was fully aspirated from the cells and 50 µL RIPA+PI was added to the first well of every condition. The well was scraped using a pipette tip and the cell lysates were passed through the pipette tip several times. When the cells of the first well were lysed, the cell lysates were pipetted up and added to the second well. The cells were lysed in the same way as the first well and so on for the third well. The combination of the cell lysates of the 3 wells was transferred to an Eppendorf and kept on ice. 300 µL 3x Laemmli sample buffer (House made, CDL UMCU, Utrecht, The Netherlands) was combined with 7.5 µL dithiothreitol (DTT) in an Eppendorf. 25 µL of the sample buffer mixture was added to 50 µL of the cell lysates. The samples were put in a heating block at 95°C for 10 min.

In the meantime, a 1x 3-(N-morpholino)propanesulfonic acid (MOPS) buffer was prepared from MOPS SDS Running Buffer (20x)(Invitrogen, Carlsbad, California, USA) by taking 20 mL of the 20x and diluting it until 400 mL with demiwater. The white strip of the Bolt™ 4-12% Bis-Tris Plus gel (Invitrogen, Carlsbad, California, USA) was removed and the gel was put in the Mini Gel Tank (Invitrogen, Carlsbad, California, USA). The MOPS buffer was added on both sides of the gel until the fill line on the Gel Tank. The comb of the gel was carefully removed. After taking the samples out of the heating block, they were put on ice to cool down. 45 µL of the samples and 7.5 µL of Precision Plus Protein All Blue Standards (Bio-Rad, Hercules, California, USA) were pipetted in the gel wells. The lid was put on the Gel Tank and attached to the voltage meter. The gel was run for 32 min at 200 V.

Meanwhile, the materials for the blot were prepared. A blotting buffer was made by adding 200 mL of 100% ethanol, 14 g of glycine and 3.03 g Tris to 800 mL demiwater. The buffer needed to be put in the fridge to be cold before use. After filling a container with blotting buffer, two sponges and two 3 mm filter papers (Cytiva, Marlborough, Massachusetts, USA) were put in it.

After the separation process, the gel was taken out of the disc and put in the container with blotting buffer. A piece of Immobilon®-FL Transfer Membrane (Merck Millipore®, Darmstadt, Germany) was cut off and activated with 100% methanol. All the components were assembled according to the instructions on the Mini Blot Module (Invitrogen, Carlsbad, California, USA). The Blot Module was placed in the Gel Tank and filled with blotting buffer after assembly. The Gel Tank was filled with demiwater around the Blot Module until the fill line. The setup was attached to the voltage meter for 60 min at 20 V.

After the transfer to the membrane was completed, the membrane was fully dried by placing it on a clean filter paper and putting it in an oven at 37°C for 10 min. The membrane was transferred to a membrane container and rehydrated with 100% methanol for 30 sec, after the drying. To rinse the membrane, TBS was added to the membrane for 5 min under gentle shaking. The membrane was rinsed with demiwater and stained with 10 mL Revert™ 520 Total Protein Stain (LI-COR® Biosciences, Lincoln, Nebraska, USA) for 5 min under gentle shaking at room temperature. After the staining, the membrane was washed two times with 10 mL Revert™ 520 Wash Solution (LI-COR® Biosciences, Lincoln, Nebraska, USA) for 30 sec under gentle shaking. The washing solution was decanted and the membrane was briefly washed with demiwater. To image the total protein staining, the membrane was analysed using an Odyssey® M in the 520 nm channel.

After imaging, 10 mL Intercept® Blocking Buffer and 10 mL TBS were added to the membrane for 2 h at room temperature under gentle shaking to block the membrane. 2.5 mL Intercept® Blocking Buffer and 2.5 mL TBS-T were added to a 50 mL tube together with 5 µL Recombinant Anti-Androgen receptor antibody (Abcam Inc, Cambridge, UK) to obtain a 1:1000 dilution of the antibody. After the 2 h blocking step, the membrane was transferred to the tube with antibody dilution. The tube was gentle rolled overnight in a cold room at 4°C. The washing step was performed the following day. This contained two washes with 20 mL TBS-T for 5 min and one wash with 20 mL

TBS for 5 min, all under gentle rolling. After the washing step, 2.5 mL Intercept® Blocking Buffer and 2.5 mL TBS-T were added to the 50mL tube with the membrane, together with 2.5 µL IRDye® 800CW Goat anti-Rabbit IgG Secondary Antibody (LI-COR® Biosciences, Nebraska, USA) for a 1:2000 antibody dilution. The tube was rolled for 1 h at room temperature, covered from light. After this incubation, the same washing step as already described was performed.

The membrane was analysed in an Odyssey® M in the 800 nm channel. To estimate the size of the detected proteins, the Precision Plus Protein All Blue Standards was used as a size reference. Using the total protein stain, the signal of the samples could be normalised to correctly compare the difference in fluorescence between samples.

3.4.7 RT-qPCR analysis

3.4.7.1 Principal

Polymerase chain reaction (PCR) is a technique where specific DNA sequences are amplified by using specific primers for this DNA sequence. A two-step RT-qPCR was used in this analysis where the reverse transcriptase and qPCR were performed separately. All of the isolated RNA from the cells was first converted to copy DNA (cDNA) using reverse transcriptase. After the conversion, qPCR was performed on the cDNA with sequence specific primers to amplify the wanted genes. (49)

A fluorescent DNA-binding dye was added to the master mix for the qPCR which could be measured by a fluorometer during the different cycles. This way a readout of fluorescence was given throughout the amplification process. Since the dye binds to DNA, an increase in amplicons results in a higher fluorescent signal. The quantification cycle (Cq) is the cycle number at which the fluorescent signal is high enough to detect. A low Cq means that there is a high amount of starting cDNA since it takes less amplification cycles for the fluorescence to be detected. This way the amount of RNA that is present in the sample can be derived. Since the signal depends on the amount of copies that are going to be generated, it is important to normalise all the samples to have the same starting amount of total RNA. That is why the RNA concentration is first measured. Another way to normalise is to include housekeeping genes as an internal reference gene. In this analysis both strategies were used to obtain a result that is as reliable as possible. (50,51)

3.4.7.2 Method

The cells were seeded and transfected with the siRNA LNPs according to the protocol described in sections 3.4.3 and 3.4.4.4. The workspace was first cleaned with RNaseZAP™ (Sigma Aldrich, Steinheim, Germany) to avoid breaking down the unstable RNA in the cells. The samples for analysis were prepared by aspirating the medium of the cells and adding 50 µL of TRIzol® LS Reagent (Life Technologies, Carlsbad, California, USA) to all the wells. The cell lysates in the wells were pipetted up and down and transferred to an Eppendorf. Since every condition was transfected in triplicate, the lysates of 3 wells with the same condition were combined in one Eppendorf.

250 µL of TRIzol® LS Reagent was added to the 150 µL of cell lysates to obtain a total volume of 400 µL. 80 µL of chloroform was added to each sample and shaken well for 15 sec. The samples were left for 2 min at room temperature before transferring them to a centrifuge at 4°C for 15 min at 12000 RPM. After centrifuging, the aqueous and organic phase were separated. Around 100 µL of aqueous phase was carefully pipetted up and transferred to a new Eppendorf together with 1 µL of GlycoBlue™ Coprecipitant (Invitrogen, Vilnius, Lithuania, USA) and 100 µL of isopropanol (Honeywell, Seelze, Germany). The samples were mixed well using a pipette and incubated at room temperature. After an incubation of 10 min, the samples were centrifuged at 4°C for 15 min at 12000 RPM. The supernatant was fully removed from the Eppendorfs and 1 mL of 75% absolute ethanol was added to the pellet. To prepare the 75% absolute ethanol solution, 100% absolute ethanol was diluted with Ambion™ DEPC-treated water (Invitrogen, Woodward St. Austin, Texas, USA). The samples were vortexed for 10 sec and centrifuged again at 4°C for 5 min at 7500 RPM. The ethanol was removed from the samples and the remaining RNA pellets were air dried for 10 min. The pellet was reconstituted in 40 µL of Ambion™ DEPC-treated water and put on ice.

The RNA concentration of the samples was measured at A260 nm by pipetting 1 µL of each sample on the sample surface of a DS-11 Spectrophotometer (DeNovix® Inc., Wilmington, Delaware, USA) after measuring Ambion™ DEPC-treated water as a blank. The volume of RNA to convert to cDNA was calculated based on the measured RNA concentration with the intention to obtain 750 ng RNA per sample. To MicroAmp® Reaction Tubes (Life Technologies, Carlsbad, California, USA) the calculated volume of the RNA samples, 4 µL iScript™ Reaction Mix (Bio-Rad Laboratories, Hercules,

California, USA) and 1 µL iScript™ Reverse Transcriptase (Bio-Rad Laboratories, Hercules, California, USA) were added and diluted with Ambion™ DEPC-treated water until 20 µL. The PCR vials were put in the GeneAmp® PCR System 2700 (Applied Biosystems, Waltham, Massachusetts, USA) with following protocol: 5 min at 25°C, 40 min at 46°C, 1 min at 95°C, hold on 4°C until taken out. After the conversion to cDNA, the samples were transferred to Eppendorfs and diluted 5 times by adding 80 µL of Ambion™ DEPC-treated water. The samples were kept at -20°C overnight.

The following day master mixes were made for the AR gene, Glyceraldehyde 3-phosphate dehydrogenase (GAPDH) and Beta-actin housekeeping genes. The master mixes were calculated with an excess of 3 samples. For every sample 12.5 µL iQ™SYBR® Green supermix, 0.1 µL forward primer, 0.1 µL reverse primer and 7.3 µL Nuclease-free water were mixed. GAPDH human paper Forward (Fw)/Reverse (Rv), Beta-actin human Fw/Rv and AR human Fw/Rv primers were ordered from Merck (Darmstadt, Germany). The sequences of these primers are given in Table 8.2.

A 96-well PCR plate (Bio-Rad Laboratories, Hercules, California, USA) was put on ice and 5 µL of every sample was dispensed in quadruplicate in the wells according to the predefined lay-out. For every master mix, a duplicate negative control was included by adding 5 µL of Nuclease-free water in stead of cDNA. 20 µL of the AR master mix was added to the samples in duplicate. 20 µL of the GAPDH and Beta-actin master mix were added in singular. It is crucial to pipette reproducibly since different volumes can result in Cq variance. The plate was covered with iCycler iQ® Optical tape (Bio-Rad Laboratories, Hercules, California, USA) and spun before placing it in the C1000 Touch™ Thermal Cycler coupled with CFX96™ Real-Time PCR detection system (Bio-Rad Laboratories, Hercules, California, USA). The program was set to 3 min at 95°C, followed by 40 cycles of 15 sec 95°C and 40 sec 60°C with a melt-curve included of 55-95°C in 0.5°C increments.

The GAPDH and Beta-actin Cq values were used to verify the validity of the samples. To analyse the results, the ΔCq was calculated for every sample using Formula (3.1).The mean of the ΔCq values were normalised based on the ΔCq value of the NT LNP.

$$\Delta Cq = 2^{-(Cq\ value\ AR - Cq\ value\ GAPDH)} \quad (3.1)$$

3.5 ASGPR1 SURFACE COATING ASSAY

3.5.1 Principal

Cell surface proteins can be detected by bringing cells in suspension first. Specific antibodies are added to the cells so the antibody can bind to its specific target protein when it is present. If the cell expresses the target protein on its surface, the cell will be coated with antibodies. Flow cytometry was performed to confirm the antibody binding to the cell, as already explained in section 3.4.5.1. The difference is that the detection of the fluorescent label is measured in the Phycoerythrin (PE)-channel, since PE labelled antibodies were used in this assay. PE has an excitation peak at 565 nm and an emission peak at 573 nm. (46)

3.5.2 Method

To detach the cells from the wells, a 10 mM EDTA (Sigma Aldrich, Steinheim, Germany) solution was used instead of Trypsin. This solution was made by dissolving 4.65 mg Na_2EDTA in water to obtain a 250 mM solution. After adjusting the pH to pH 6.5 with HCl, the 250 mM EDTA solution was further diluted until 10 mM with DPBS. (52)

24h prior to the assay, HepG2 and HEK293FT were seeded with a density of 50000 and 24000 cells/well respectively, as mentioned in section 3.4.3. The medium of the wells was aspirated and the wells were washed with 200 µL DPBS and 50 µL 10 mM EDTA was added to the cells. After a 10 min incubation at 37°C, 100 µL DPBS 2% Bovine Serum Albumin (BSA)(Sigma-Aldrich, Steinheim, Germany) was added to the wells. The cells were resuspended and transferred to an Eppendorf. After centrifuging the cells for 5 min at 300 RPM, the supernatant of the Eppendorf was aspirated and 100 µL DPBS 2% BSA was added to the wells. Three different concentrations of antibodies were compared in this assay. 5 µL, 10 µL and 20 µL of Phycoerythrin (PE) mouse anti-ASGPR 1 (BD Bioscience, Franklin Lakes, New Jersey, USA) were added to 3 separate Eppendorfs. As controls, 20 µL, 40 µL and 80 µL of PE mouse IgG1 kappa isotype control (BD Bioscience, Franklin Lakes, New Jersey, USA) were added to the remaining 3 Eppendorfs. The cells were carefully vortexed and incubated with the antibodies for 30 min on ice. From now on, the cells were at all times protected from light.

After the 30 min incubation, the Eppendorfs were centrifuged for 5 min at 300 RPM to spin the cells down. The supernatant was aspired to remove the unbound

antibody. The cells were resuspended again with 200 µL DPBS 2% BSA and centrifuged for 5 min at 300 RPM. The supernatant was aspirated and 200 µL of DPBS 2% BSA was added to the Eppendorfs. The cells were resuspended and transferred to a flat-bottom 96-well FACS plate for analysis. (53,54)

The gatings were set to match the single cells. The mean PE-Area value of the anti-ASGPR 1 was divided by the mean PE-Area value of the isotype control. These values were plotted in a graph.

4 RESULTS

4.1 LNP CHARACTERISATION

4.1.1 Particle size and PdI

4.1.1.1 In situ mRNA LNP

The average particle size and mean PdI value of the NT LNP, 0.25%, 0.5% and 1% GalNAc LNPs were 96.8, 89.8, 82.6 and 80.4 nm and 0.230, 0.254, 0.145 and 0.072 respectively, as could be seen in Figure 4.1. An increase in GalNAc molar ratio resulted in a smaller particle size. There was a 16.4 nm difference when comparing the size of the NT LNP and 1% GalNAc LNP. Nevertheless the particle size of the LNPs stayed within the range of 60 nm and 100 nm. The PdI of all the LNPs was under 0.3. The 1% GalNAc LNP even had a PdI lower than 0.1.

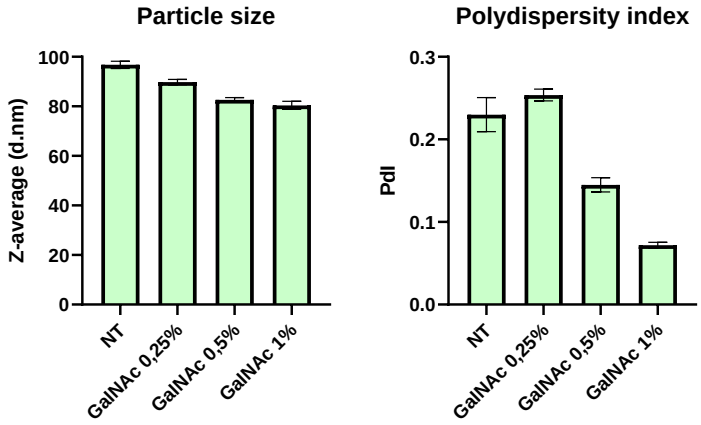

Figure 4.1: The average diameter of the LNPs given in nm (left) and the average polydispersity index (right) measured by DLS. The investigated samples are the non-targeted LNP and in situ GalNAc LNPs with molar ratio ranging from 0.25% to 1% encapsulated with Cy 5-eGFP mRNA.

4.1.1.2 Post-insertion mRNA LNP

The average particle size and mean PdI value of the NT LNP, 0.25%, 0.15% and 0.05% GalNAc LNPs were 82.4, 80.1, 79.6 and 78.8 nm and 0.153, 0.129, 0.153 and 0.122 respectively, as given in Figure 4.2. The size of the LNPs was similar and under 100 nm. The PdI fluctuated between 0.12 and 0.16.

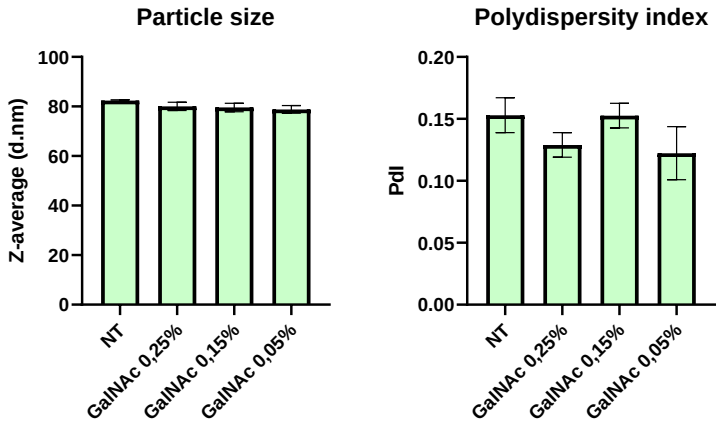

Figure 4.2: The average diameter of the LNPs given in nm (left) and the average polydispersity index (right) measured by DLS. The investigated samples are the non-targeted LNP and post-inserted GalNAc LNPs with molar ratio ranging from 0.05% to 0.25% encapsulated with Cy 5-eGFP mRNA.

4.1.1.3 siRNA LNP

The average particle size and mean PdI value of the NT LNP and 0.25 GalNAc LNP were 63.8 and 63.9 nm and 0.127 and 0.111 respectively, as mentioned in Figure 4.3. The particle size of both LNPs was almost identical with a difference of 0.1 nm. The PdI ranged between 0.1 and 0.13.

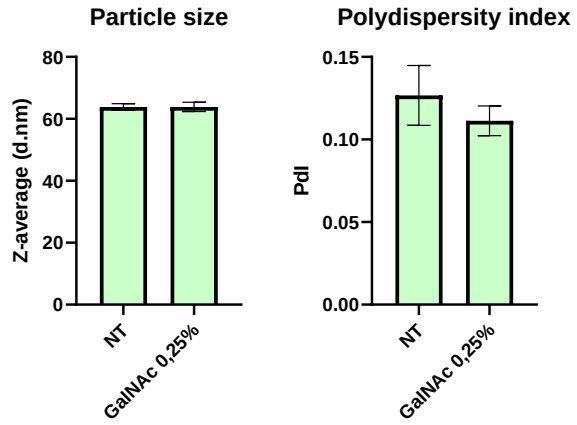

Figure 4.3: The average diameter of the LNPs given in nm (left) and the average polydispersity index (right) measured by DLS. The investigated samples are the non-targeted LNP and in situ GalNAc LNPs with molar ratio 0.25 % encapsulated with AR siRNA.

4.1.2 RiboGreen assay

4.1.2.1 In situ mRNA LNP

The determined encapsulation efficiency was 97.21%, 97.25%, 96.95% and 96.88% for NT LNP, 0.25%, 0.5% and 1% GalNAc LNPs respectively, as seen in Figure 4.4. The LNPs showed similar encapsulation efficiencies, all well above 90%.

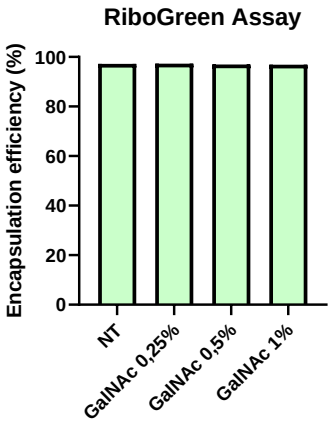

Figure 4.4: The calculated encapsulation efficiency of the LNPs given in percentage measured by the RiboGreen Assay. The investigated samples are the non-targeted LNP and in situ GalNAc LNPs with molar ratio ranging from 0.25% to 1% encapsulated with Cy 5-eGFP mRNA.

4.1.2.2 Post-insertion mRNA LNP

The determined encapsulation efficiency was 96.23%, 97.26%, 97.43% and 97.97% for NT LNP, 0.25%, 0.15% and 0.05% GalNAc LNPs respectively. The encapsulation efficiencies were similar for all the LNPs, as can be seen in Figure 4.5.

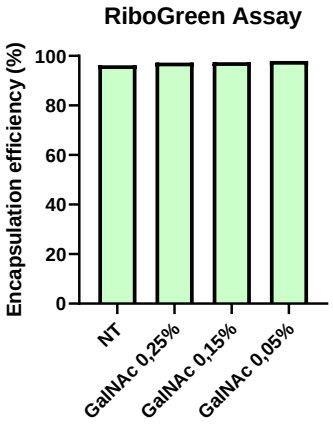

Figure 4.5: The calculated encapsulation efficiency of the LNPs given in percentage measured by the RiboGreen Assay. The investigated samples are the non-targeted LNP and post-inserted GalNAc LNPs with molar ratio ranging from 0.05% to 0.25% encapsulated with Cy 5-eGFP mRNA.

4.1.2.3 In situ siRNA LNP

The determined encapsulation efficiency was 93.14% and 90.44% for NT LNP and 0.25% GalNAc LNP respectively (Figure 4.6). The encapsulation efficiency of both LNPs were on the lower side compared to the mRNA LNPs but were still above 90%.

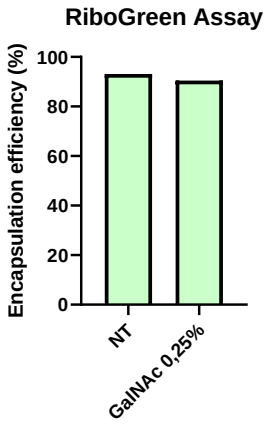

Figure 4.6: The calculated encapsulation efficiency of the LNPs given in percentage measured by the RiboGreen Assay. The investigated samples are the non-targeted LNP and in situ GalNAc LNPs with molar ratio 0.25% encapsulated with AR siRNA.

4.1.3 Dot blot

A dot blot was performed according to the method in section 3.2.3 for all the LNPs made with Cy 5 labelled eGFP mRNA. The measured fluorescence at 488 nm can be seen in Figure 4.7. A fluorescent signal was detected for both the post-insertion LNPs and in situ LNPs with GalNAc with an exception of the post-insertion 0.05% GalNAc LNP. The positive control, GalNAc-PEG, showed a bright signal. The spots with NT LNPs and PBS did not show a signal. The LNPs with a lower molar ratio of GalNAc produced a faint signal compared to the higher ratios.

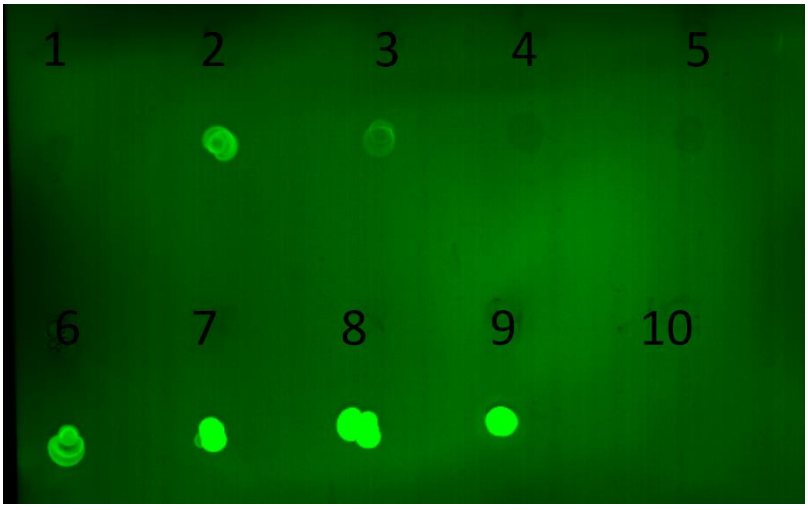

Figure 4.7: Results of dot blot with Cy 5 labelled eGFP mRNA LNPs with fluorescence measured at 488 nm. 1= NT LNP made for the post-insertion batch, 2= post-insertion 0.25% GalNAc LNP, 3= post-insertion 0.15% GalNAc LNP, 4= post-insertion 0.05% GalNAc LNP, 5= NT LNP made for the in situ batch, 6= In situ 0.25% GalNAc LNP, 7= In situ 0.5% GalNAc LNP, 8= In situ 1% GalNAc LNP, 9= GalNAc-PEG, 10= DPBS

4.2 ASGPR 1 SURFACE COATING ASSAY

Both HepG2 and HEK293FT were analysed as described in section 3.5 with 3 different concentrations: 1x, 2x and 4x the manufacturer's recommended concentration. The signal of the specific ASGPR 1 antibody was normalised based on the isotype control signal. The normalised signal is given in Figure 4.8 for the different concentrations.

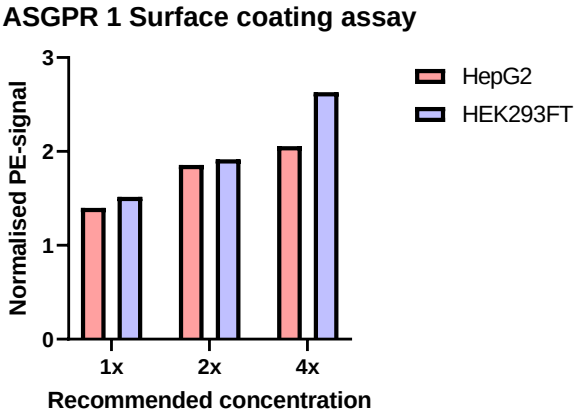

Figure 4.8: ASGPR 1 surface coating assay FACS results for HepG2 and HEK293FT. The specific antibody signal was normalised by the isotype control for different concentrations according to the recommended concentration by the manufacturer.

HepG2 and HEK293FT showed a similar signal for ASGPR 1 specific antibody for the three concentrations. A higher concentration of antibody resulted in a stronger signal for both cell lines.

4.3 TRANSFECTION ASSAY

4.3.1 Transfection Protocol 1

HepG2 and HEK293FT were transfected as mentioned in section 3.4.4.2 with Cy 5 labelled eGFP mRNA LNPs. Seven different conditions were tested. PBS was included as negative control to account for background. The NT LNP, Apo E LNP and in situ GalNAc LNPs were tested in this assay. The results of the FACS analysis are given in Figure 4.9. The signal was normalised on the signal obtained from the NT LNP.

The uptake of the LNPs with Apo E increased by a factor of 10.46 for HepG2 and 19.82 for HEK293FT. The transfection only increased by 1.42 and 1.57 for HepG2 and HEK293FT for the Apo E LNPs.

The uptake for the 0.25% GalNAc LNP increased by 1.3 and 1.2 for both cell lines. The 0.5% GalNAc LNP showed an uptake similar to the NT LNP. The uptake of

the 1% GalNAc LNP was reduced to 0.46 and 0.52. As already stated, the PBS sample functions to account for the background signal. The transfection signals of the GalNAc LNPs were similar to the PBS sample, meaning they showed little to no transfection.

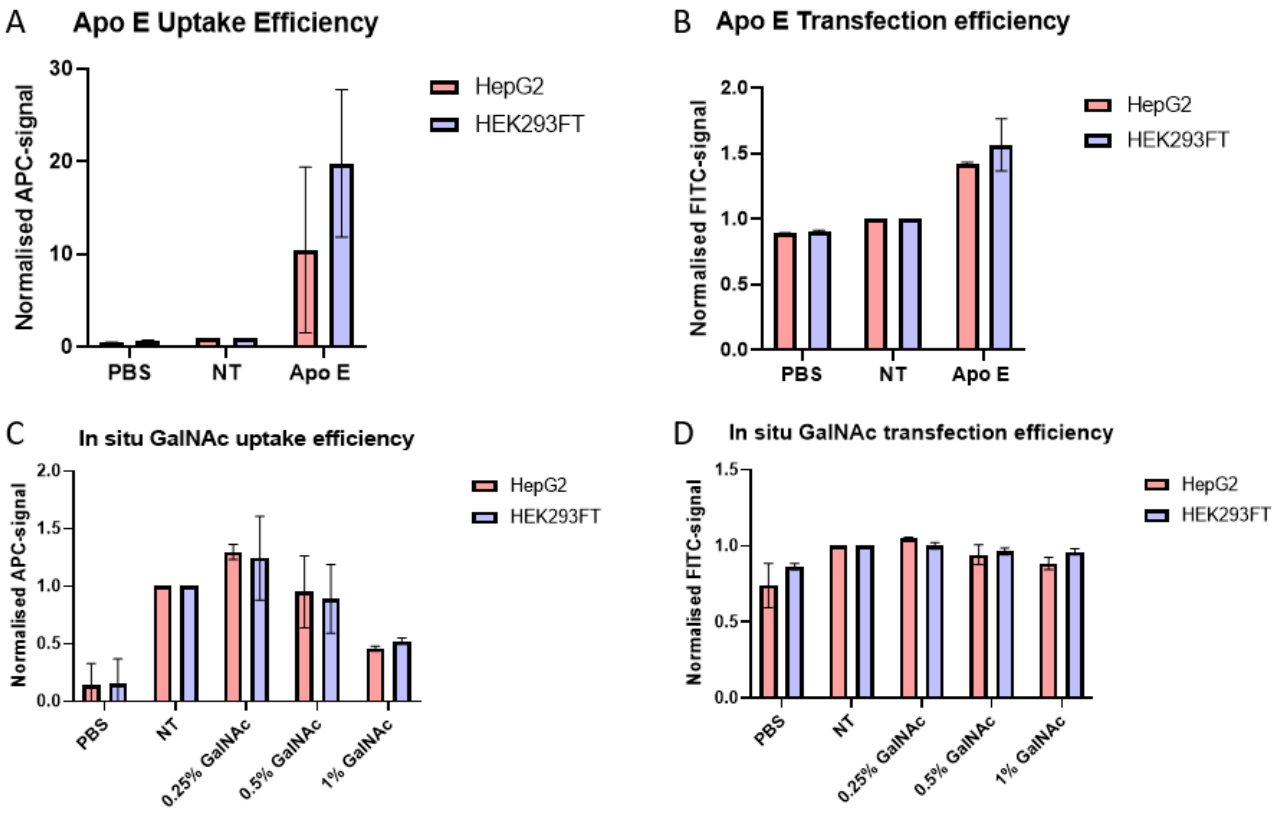

Figure 4.9: FACS results for the first transfection protocol with HepG2 and HEK293FT. The uptake (A) and transfection (B) normalised by the NT LNP signal for the Apo E experiment with samples PBS control, NT LNP and Apo E LNP. The uptake (C) and transfection (D) normalised by the NT LNP signal for the GalNAc experiment with samples PBS control, NT LNP and in situ GalNAc LNPs with molar ratio ranging from 0.25% to 1%. All the LNPs were encapsulated with Cy 5 labelled eGFP mRNA.

4.3.2 FACS analysis

4.3.2.1 Apo E experiments

Both cell lines were transfected according to the protocol in section 3.4.4.3 with PBS, NT LNP and Apo E LNPs containing Cy 5 labelled eGFP mRNA. The FACS results were normalised based on the NT LNP signal. The mean of these values was calculated for 5 repetitions of the experiment and given in Figure 4.10.

Apo E caused an increase of 9.39 in LNP uptake in HepG2 cells and an 10.91 increase for HEK293FT cells. The transfection increased by 6.82 and 12.17 for HepG2 and HEK293FT respectively. All the mentioned increases were found to be statistically significant.

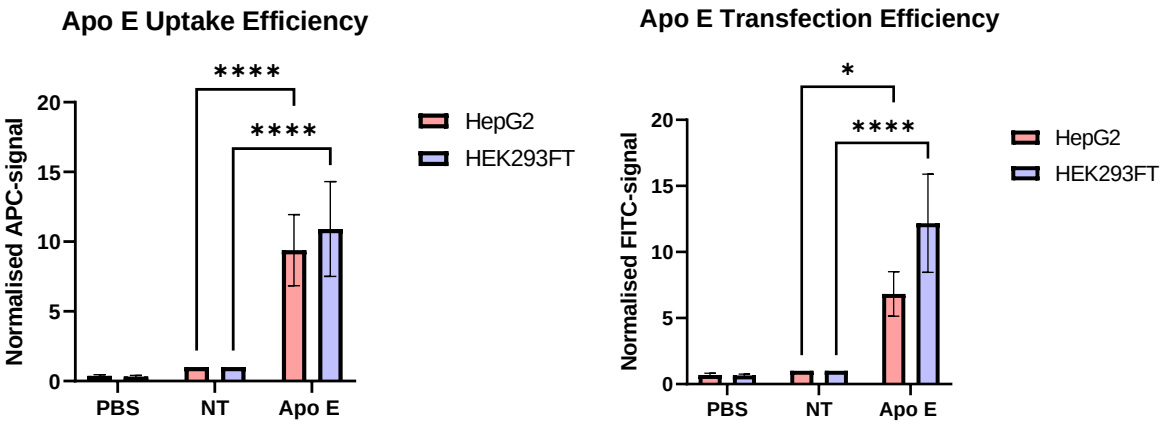

Figure 4.10: FACS results of transfection assay with protocol 2 of HepG2 and HEK293FT with Cy 5 labelled eGFP mRNA LNPs. The uptake (left) and transfection (right) normalised by the NT LNP signal for the Apo E experiment with samples PBS control, NT LNP and Apo E LNP.

4.3.2.2 GalNAc experiments

According to the protocol in section 3.4.4.3, HepG2 and HEK293FT were transfected with PBS, NT LNP and GalNAc LNPs containing Cy 5 labelled eGFP mRNA. The FACS signals normalised on the NT LNP were calculated. The means of the normalised signal of 3 repetitions with in situ GalNAc LNPs with molar ratios 0.25%, 0.5% and 1% are given in Figure 4.11.

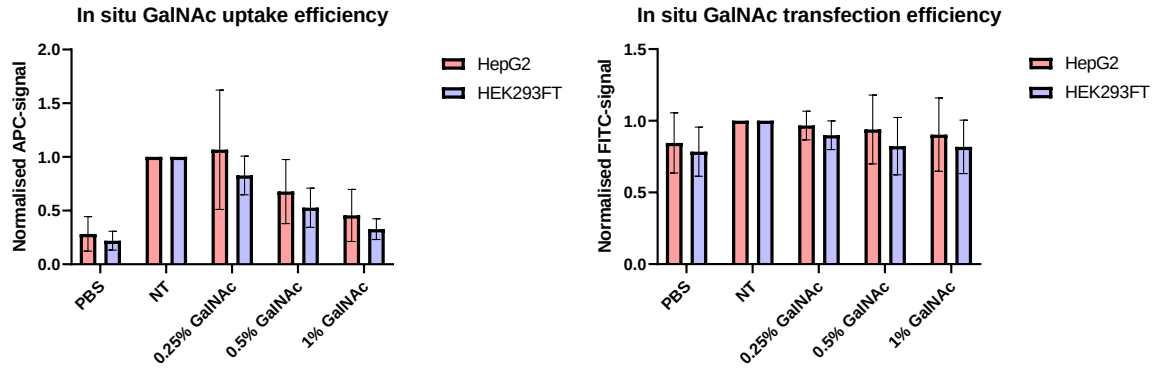

Figure 4.11: FACS results of transfection assay with protocol 2 of HepG2 and HEK293FT with Cy 5 labelled eGFP mRNA LNPs. The uptake (left) and transfection (right) normalised by the NT LNP signal for the GalNAc experiment with samples PBS control, NT LNP and in situ GalNAc LNPs with molar ratio ranging from 0.25% to 1%.

The uptake of the in situ 0.25% GalNAc LNP increased by a factor of 1.07 for the HepG2 cells and decreased by 0.83 for HEK293FT. In situ 0.5% and 1% GalNAc LNPs had a negative effect on the uptake of the LNPs for both cell lines. Larger amounts of GalNAc resulted in a decrease in uptake signal. The transfection of the in situ GalNAc

LNPs and NT LNP was similar to the PBS control. This suggested little to no transfection of the eGFP mRNA.

The mean of the normalised signal of 2 repetitions with post-inserted GalNAc LNPs containing Cy 5 labelled eGFP mRNA with molar ratios 0.25%, 0.15% and 0.05% can be seen in Figure 4.12. The post-insertion GalNAc LNPs had a similar effect on the uptake for HepG2. The uptake in HEK293FT was negatively influenced by the GalNAc LNPs since the signal was almost halved compared to the NT LNP. The transfection of the mRNA was negatively influenced by the GalNAc LNPs for both cell lines.

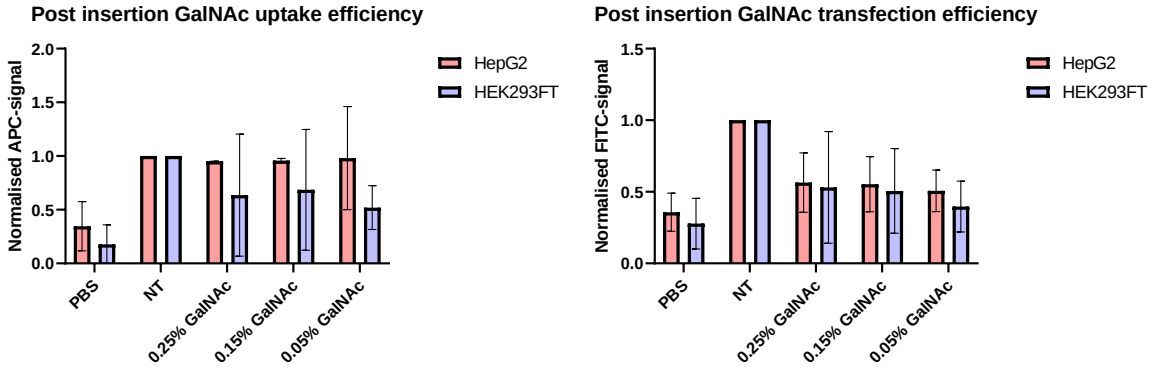

Figure 4.12: FACS results of transfection assay with protocol 2 of HepG2 and HEK293FT with Cy 5 labelled eGFP mRNA LNPs. The uptake (left) and transfection (right) normalised by the NT LNP signal for the GalNAc experiment with samples PBS control, NT LNP and post-inserted GalNAc LNPs with molar ratio ranging from 0.05% to 0.25%.

4.3.3 Western blot analysis

HepG2 and HEK293FT were transfected as mentioned in section 3.4.4.3. with AR siRNA LNPs. The tested conditions in this assay were PBS, NT LNP, Apo E LNP and in situ 0.25% GalNAc LNP. A sample of untreated cells was included for both cell lines as an additional negative control. The assay was performed with and without addition of MG-132 16 hours prior to lysing the cells. 48 hours post-transfection the cells were lysed and run on western blot. The western blot membranes given in Figure 4.13 were analysed at 800 nm.

There were no bands visible around the size of 110 kDa. For all the samples, there are bands noticeable at 37 kDa. The same results can be seen with or without addition of MG-132.

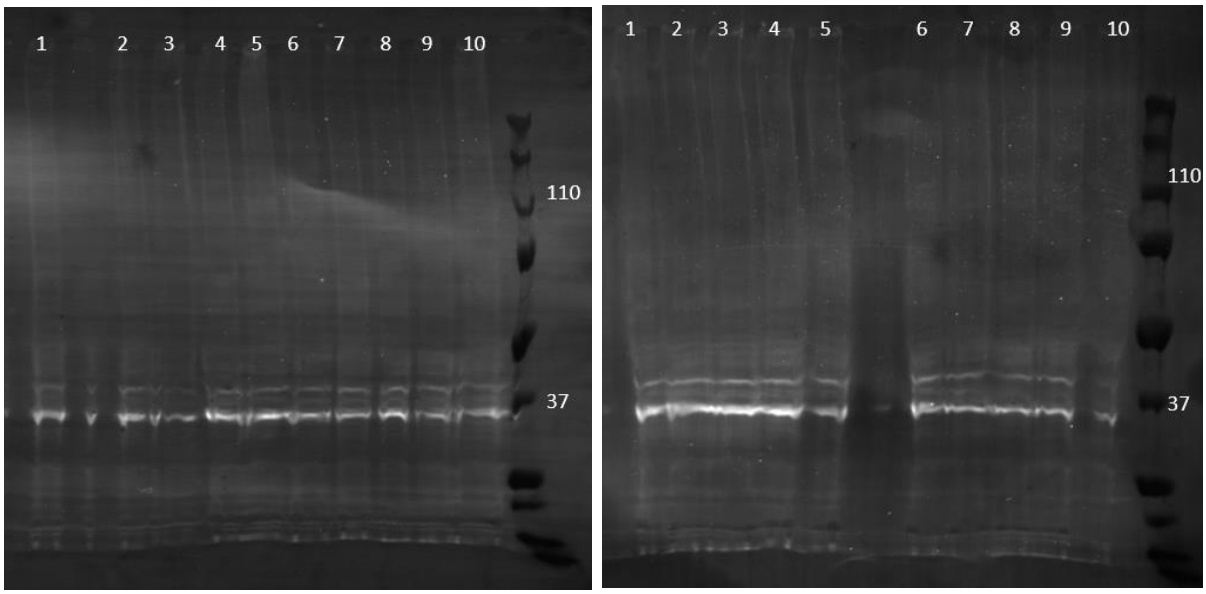

Figure 4.13: Western blot of the cell lysates of HepG2 and HEK293FT transfected with AR siRNA LNPs without MG-132 addition (left) and with MG-132 addition (right). The fluorescence was measured at 800 nm. 1= HepG2 transfected with PBS, 2= HepG2 transfected with NT LNP, 3= HepG2 transfected with Apo E LNP, 4= HepG2 transfected with in situ 0.25% GalNAc LNP, 5= untreated HepG2, 6= HEK293FT transfected with PBS, 7= HEK293FT transfected with NT LNP, 8= HEK293FT transfected with Apo E LNP, 9= HEK293FT transfected with in situ 0.25% GalNAc LNP, 10= untreated HEK293FT

4.3.4 RT-qPCR analysis

HepG2 and HEK2933FT were transfected according to the protocol in section 3.4.4.3 with AR siRNA LNPs. The tested conditions were PBS, NT LNP, Apo E LNP and in situ 0.25% GalNAc LNP. From the obtained Cq value, the ΔCq-value was calculated with Formula (3.1). The ΔCq-values were normalised based on the NT LNP ΔCq-value.

The included negative controls gave a non detectable signal. The Cq values of the AR gene for HepG2 ranged from 32.8 for the PBS sample to 37.5 for the Apo E LNP sample. The HEK293FT PBS sample had a Cq value of 29.7 for the AR gene.

The Apo E samples for the HEK cell line were excluded from the analysis due to large deviations of the Cq value of the housekeeping genes from the other samples, as can be seen in Figure 4.14. The Cq value of the housekeeping genes for the other samples were similar.

For HepG2 the ΔCq-value of the Apo E sample was 0.35, which resembles an additional silencing of 65% compared to the NT LNP, as can be seen in Figure 4.15. The silencing for the PBS and 0.25% GalNAc sample in HepG2 were similar with

respective values of 5.14 and 6.40. The gene silencing in HEK293FT was less efficient than the silencing in HepG2 since the difference between PBS and the NT LNP is smaller.

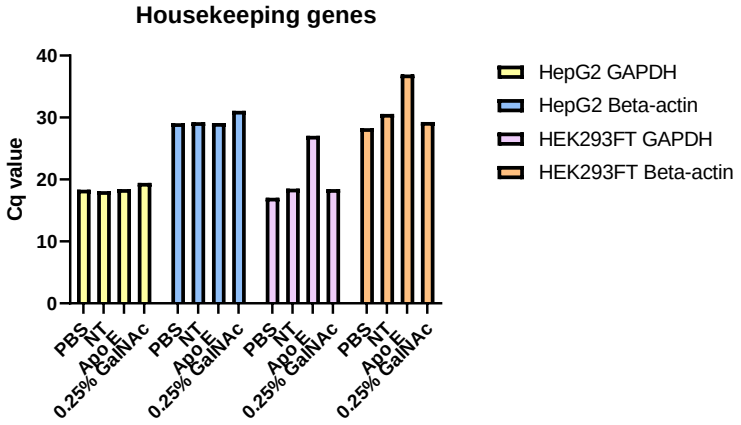

Figure 4.14: RT-qPCR results of Cq value of housekeeping genes GAPDH and Beta-actin in HepG2 and HEK293FT. The Cq value is given for PBS control, NT LNP, Apo E LNP and in situ 0.25% GalNAc LNP samples.

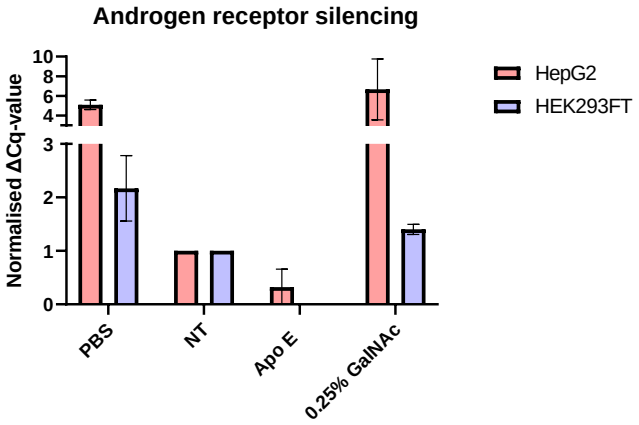

Figure 4.15: RT-qPCR results of HepG2 and HEK293FT transfected with AR siRNA. The ΔCq value was normalised by the NT LNP with samples PBS control, NT LNP, Apo E LNP and in situ 0.25% GalNAc LNP.

5 DISCUSSION

5.1 LNP CHARACTERISATION

5.1.1 Post-insertion Apo E LNPs

Because the protocol for the post-insertion of the Apo E LNPs did not include a dialysis step, possible unbound Apo E was not removed. It is possible that not all the Apo E was incorporated in the LNPs. A dialysis of the LNPs could remove this uncertainty. Unbound Apo E could possibly occupy the LDLR, resulting in a negative influence on the results.

According to literature Apo E is nicely incorporated into the LNPs as mentioned in section 1.6.1. Nevertheless, it would be advised to include an additional characterisation to verify if the Apo E was truly incorporated into the LNP. A dot blot or electron microscopy could be used to test this. Given the results of the FACS analysis, it could be concluded that Apo E was indeed present on the surface of the LNPs.

5.1.2 Particle size and PdI

All the LNPs showed a particle size between 60 and 100 nm, which is the preferred range. The PdI of all the LNPs was lower than 0.3, confirming a sufficient homogeneity. The 1% in situ GalNAc LNP even showed a PdI under 0.1, which suggests monodispersity. (37)

For the in situ made GalNAc LNPs, a higher molar ratio of GalNAc resulted in a lower particle size. This was unexpected since GalNAc-PEG has a higher molar weight than DMG-PEG2000. Although, this could be explained by the differences in behaviour of the added lipids. DMG-PEG2000 can possibly interact with the other lipids and the aqueous phase in a different way than GalNAc-PEG, resulting in different particle sizes.

5.1.3 RiboGreen assay

The encapsulation efficiency was above 90% for all the LNPs, which complies with the requirements. This indicates that there was a low fraction of free RNA present in the LNP-buffer solution, which means that the majority of the RNA was encapsulated in the LNPs.

5.1.4 Dot blot

Both the post-insertion and the in situ GalNAc LNPs showed a signal on the membrane. This suggests that GalNAc was available on the surface of the LNPs. The LNPs who were post inserted with 0.05% GalNAc did not show any signal. This can be

explained by the fact that sWGA is not a lectin specifically for GalNAc. sWGA binds specifically to N-acetyl-glucosamine (GlcNAc). However, the lectin showed enough cross-reactivity with GalNAc to react with the higher molar ratios but not enough for lower concentrations such as 0.05%. (55)

A dot blot is a semi-quantitative assay meaning that the quantitative ratio of GalNAc on the LNP surface could not be determined. Regardless of this fact, 0.15% and 0.25% GalNAc show a fainter signal compared to 0.5% and 1%. This suggests a lower GalNAc concentration for the 0.25% and 0.15% LNPs. The aim of the experiment was to show that GalNAc was present on the surface and not to check if the molar concentration was correct. The semi-quantitative aspect of this assay does not pose a problem in that way.

A potential problem in this assay is the possibility that the LNP gets lysed when spotted on the membrane or because of the Tween in TBS-T. This could result in a false positive for the in situ GalNAc LNPs. No matter if the GalNAc-group is present on the surface of the LNP or inside, if the LNP gets lysed, it will give a positive result. However, this does not pose a problem for the post-inserted GalNAc LNPs. If GalNAc is present in these samples, it must be because they are on the surface since GalNAc was not present when the LNPs where formulated. The LNPs were also dialysed after post-insertion so all the free unbound GalNAc was removed. To completely rule out the possibility of a false positive, the LNPs could be incubated with sWGA in suspension so it can properly bind to the surface. After this incubation sWGA could be washed away by dialysis for example and after this step the LNPs could be spotted in the membrane. This might give a more reliable result for the in situ made LNPs.

5.2 ASGPR 1 SURFACE COATING ASSAY

HepG2 cells are supposed to be one of the highest expressing ASGPR 1 cell lines. However, it can never be ruled out that the cells start behaving differently and lose the expression of certain receptors. This can certainly happen when cells get a higher passage number, which was the case for the used HepG2 cells. Since the GalNAc experiments do not show convincing positive results, the cells were checked for their expression of ASGPR 1.

The use of the isotype control is to account for the aspecific binding of the antibody. Because it can not show for 100% what the aspecific binding of the antibody will be, it can only give a good indication. It could be that the increase in signal that can

be seen with higher concentrations, is just aspecific binding that the isotype control is not accounting for. This becomes even more plausible because of the same increase for the HEK293FT cells. The HEK cells do not express ASGPR 1 so they are a good negative control for this assay.

Another possibility is that the antibody was not working. The assay was executed twice with different batches of antibody. Both assays gave similar results. Unless both antibodies were faulty, the problem could not be with the antibody.

The issue with this assay on the other hand is that there was no good positive control available. Including cells with a confirmed ASGPR 1 expression would have given a good notion of what a positive signal looks like to properly compare the results. According to the manufacturer's website, there should be an increase of 100x for the specific antibody compared to the isotype control. (56) If this is an indication of how much the signal should increase, the assay is negative.

The results of this assay suggested that the HepG2 cells did not express ASGPR 1 but no hard conclusions can be drawn from this because of the lack of a positive control. Repeating this assay when a good positive control is available can be a solution.

5.3 TRANSFECTION ASSAYS

5.3.1 Transfection Protocol

Protocol 1 as described in section 3.4.4.2 was first used to investigate the influence of Apo E on the uptake of the LNPs. Although the FCS in the used media to culture the cells is heat inactivated, which should denature all the proteins inside such as Apo E, no treatment is 100% effective. It could be possible that there are still remnants of Apo E in the FCS. For this reason the first protocol was designed to avoid FCS as much as possible. That is why the cells were first washed with PBS to remove the remains of medium and afterwards only Opti-MEM® without FCS was used. The PBS washing at the end had the purpose of removing possible LNPs that were still present. The issue with this protocol is that even though the uptake of the LNPs was decent, the transfection was barely above background. A possible explanation is that the cells were starving by being in Opti-MEM® for this long and were trying to survive by not expressing additional proteins such as the eGFP protein. Another explanation might be that they did express the eGFP protein at first but used it as nourishment because they were starved. Another downside of this protocol was the extensive

washing steps, which caused a large loss of cells. As already mentioned before, the cells tended to detach very easily. So it was better to limit the operational steps to the cells.

For these reasons, the protocol was optimized and resulted in protocol 2 as described in section 3.4.4.3. There were no more washing steps and the cells got DMEM +/+ again after 6h incubation with the LNPs. This way, there was less cell loss and the cells had enough nutrients to grow and express proteins after uptake of the LNPs. The background signal can be higher with the second protocol but since the values were normalised by the NT LNP, the background was taken into account.

5.3.2 FACS analysis

5.3.2.1 Apo E experiments

Apo E seemed to increase the uptake and transfection in HepG2 cells, which suggests an in vitro hepatocyte targeting. A similar increase in uptake and transfection could be seen in HEK293FT cells, even though they express little LDLR. This could be explained by the fact that HEK cells are highly metabolic and transfectable cells. This is certainly the case for the “FT” cells, since this is a fast growing variant of the normal HEK293T. HEK cells do have a low expression of LDLR so it is possible that over time the HEK cells mutate and develop a higher expression of LDLR. Other receptors can also make use of Apo E for the uptake of LNPs, which could partially explain the similar increase for HEK293FT cells. Choosing a cell line that has a knockout for the LDLR as a negative control is a possible extension to better prove the targeting by Apo E.

5.3.2.2 GalNAc experiments

There was a slight increase in the uptake for 0.25% GalNAc in situ LNPs but the standard deviation for this sample was high. Since the transfection also did not increase, the results of this experiment did not look positive. The eventual goal of the project is to show silencing of genes, for which transfection of the RNA is essential. It could be seen that the higher the molar ratio got, the worse the uptake and transfection got. This suggests that there is an optimum at 0.25% for the ratio of GalNAc incorporated in the LNPs.

The LNPs were made with the GalNAc group already incorporated in the lipid phase. Since it is not really known how the lipids precisely interact with each other while the LNPs are formed, it is unknown where the GalNAc functional groups end up. It could be possible that the GalNAc groups were not all present on the surface but partially on the inside with the functional group for example. For this reason, additional

LNPs were made where GalNAc was post inserted. This way, the functional group should for sure be on the surface. Because there seemed to be an optimum in the molar ratio of GalNAc, lower ratios were tested with the post-insertion method to examine if an even lower ratio could be more beneficial.

The uptake of the post inserted LNPs was similar to the NT LNP for the HepG2 cells. A targeting effect could not be seen for the post-inserted LNPs. The post-insertion even seemed to have a negative effect on the transfection of the mRNA compared to the NT LNP. The negative effect that can be seen on the transfection might be explained by the higher ratio of PEG in the post-insertion LNPs. In the in situ LNPs, there is a total molar ratio of 1.5% PEG present. In the post-insertion ones on the other hand, there is an extra fraction of PEG added with the GalNAc-PEG. As already stated in section 1.5.2, a high PEG-concentration negatively influences the transfection.

The data suggests that the GalNAc targeting does not work or even has a negative influence on uptake as well as transfection of the LNPs. Since the used HepG2 cells did not seem to express the ASGPR 1 as seen in section 4.2, conclusions on this matter could not be drawn. GalNAc conjugation to NAT has been proven to work as mentioned in section 1.6.2. This could not be demonstrated with the available cells, since the results that were obtained here are not reliable enough. It is recommended to repeat the experiments with new HepG2 cells or another kind of hepatocarcinoma cell line such as Hep3B. HepG2 is the hepatocarcinoma cell line with the highest expression of ASGPR 1 but since Hep3B also expresses these receptors, they could also be useful to test the LNPs with. Since the in situ made LNPs show a better result, it would be good to try the lower molar ratios of the post-insertion LNPs with the formulation method of the in situ LNPs.

5.3.3 Western blot analysis

The androgen receptor has a size of 110 kDa. Around this size, bands were not noticeable. This suggests that the receptor is not visible on the western blot, not even for the untreated cells. There were bands visible around 37 kDa for both cell lines. This could be splice variants or breakdown products of the receptor. There are no known splice variants of the receptor around this size, making this line of thought less plausible. The best explanation for these bands would be aspecific binding of the primary antibody.

Another explanation for the lack of signal could be that HepG2 and HEK293FT have a low expression of the androgen receptor. Western blot detection for the AR is mostly used for prostate cancer cell lines, which have a much higher expression of the AR in comparison to hepatocarcinoma cells. It could be possible that the used protein concentration was too low to show signal for the HepG2 and HEK293FT cells. A potential solution to increase the protein concentration is to use more cells or to use protein extractions as samples instead of whole cell lysates. These protein extractions could be obtained by using immunoprecipitation for example. This way the protein concentrations that are brought on the gel, would be higher and might show signal. In this assay the protein concentration was increased by adding MG-132 to the cells. By inhibiting the breakdown of the androgen receptor, this protein would pile up inside the cells and result in a higher concentration when lysing them. In literature this has been tested and showed good results to increase the protein amount in HepG2 cells. (57) Since this approach also led to negative results on the western blot, the protein concentration was still not high enough to detect. Both cell lines do show an expression of the receptor as an AR specific signal could be picked up by RT-qPCR (4.2.4). Thus, the absence of AR in the cells could not be the reason why the western blot was not working.

Another explanation could be that the used antibody did not work properly. Including a positive control would be a good solution to verify this. A good cell line to have included is LNCap for example, which is a prostate cancer cell line with a high expression of the AR. If these cells show up in the western blot, the function of the antibody could be confirmed.

For all previous reasons, it was not possible to draw any conclusion on the working or targeting of the siRNA LNPs by western blot. Using siRNA against the CerS or DEGS gene would have been more ideal. This could prove that the silencing of these genes results in a lower expression of ceramide. Because both of these siRNAs were not available in the lab, AR siRNA was used. Even though AR siRNA was not an ideal choice for the HepG2 cells, the objective remained to demonstrate whether the targeting of the LNPs worked or not.

5.3.4 RT-qPCR analysis

Since the western blots came out negative, the silencing of the LNPs was tested on mRNA level with RT-qPCR instead of on protein level. The Apo E sample for

HEK293FT was excluded from the analysis because of deviating values for both housekeeping genes. Technical issues might have occurred such as pipetting errors which caused a non-reliable result. The housekeeping gene Cq-values of the other samples were similar.

There was no signal detectable for the negative controls, which makes the results of the samples even more reliable since there were no primer dimers amplified. This suggests that the detected signal of the samples was only caused by the cDNA itself.

The Cq-values of the PBS samples for both cell lines were quite high, which suggests a low expression of the AR receptor on the cells. This can explain why the detection using western blot did not work. Western blot was not sensitive enough to show the AR proteins in these low concentrations. Since RT-qPCR is much more sensitive, results could be obtained with this method.

Since the 0.25% GalNAc in situ LNP showed slightly positive uptake signals in the FACS analysis, it was included in both this experiment and the western blot. For HepG2 the 0.25% GalNAc sample had a higher ΔCq-value than the PBS sample. This should not be possible since the expression could theoretically not get higher than the control sample. Since the 0.25% GalNAc sample had a high standard deviation, the difference with the PBS sample could be explained by small pipetting errors. It is possible that the signal was around the same as the PBS signal. This would mean that the GalNAc LNP had a small to no effect on the silencing of the gene.

Apo E LNPs seem to have an additional silencing effect of 65% on top of the silencing of the NT LNP for HepG2. Since only one experiment was performed, repetitions would be advised to verify if similar results keep being obtained. Especially because the Apo E sample of HEK293FT was excluded, which made comparisons with HepG2 impossible. Nevertheless this implies promising results regarding the Apo E targeting.

6 CONCLUSION

The focus of this paper was directed towards the in vitro liver targeting using two different approaches, Apo E and GalNAc conjugation to LNPs. These targeted LNPs were tested with both Cy 5 labelled eGFP-mRNA and AR siRNA encapsulated.

The produced LNPs were characterised beforehand on particle size, PdI and encapsulation efficiency. All the LNPs complied according to the predefined criteria. The LNPs had a size between 60 and 100 nm, a PdI lower than 0.3 and an encapsulation efficiency above 90%. The GalNAc LNPs were additionally characterised for the presence of GalNAc on the LNP surface. It was found that the GalNAc functional groups were present on the LNP surfaces for the in situ made LNPs as well as the post-inserted LNPs.

The transfection protocol was optimized to have the best conditions for the cells to take up and transfect LNPs. Transfection assays of the Cy 5 labelled eGFP-mRNA LNPs were first investigated. The uptake and transfection of Apo E LNPs showed a significant increase in comparison to the NT LNPs for both HepG2 and HEK293FT. The increase suggests a hepatocyte targeting. However, using a knockout cell line as a negative control in stead of HEK293FT could give a more reliable result on the hepatic specificness of Apo E. The GalNAc LNPs did not show an improved uptake nor transfection in the cell lines. Since the results of the ASGPR surface coating assay suggested a negative result for the ASGPR 1 expression on the HepG2 cells, conclusions concerning the GalNAc targeting could not be drawn. To investigate the GalNAc targeting, it would be advised to test other hepatocarcinoma cells with a confirmed expression of ASGPR 1. Even though the targeting of GalNAc could not be proved, an optimum in GalNAc molar ratio in the LNPs could be established for 0.25%. It was noticed that incorporating GalNAc in the lipid phase of the LNPs displayed a more positive result than the post-inserted LNPs.

The targeting was further investigated for gene silencing with AR siRNA. Silencing on protein level could not be shown on western blot since the expression of the AR on both cell lines was too low for detection using this technique. Even a treatment with a protease inhibitor, MG-132, was not sufficient to increase the protein concentration to a detectable amount. Through RT-qPCR a signal for the AR could be picked up. With this technique a 65% additional silencing for the Apo E LNP could be shown in comparison to the NT LNP for HepG2. Due to technical errors, a HEK293FT

control sample for this LNP was not available. AR siRNA was not an ideal choice of siRNA but it was able to show the targeting effect of the LNPs. It would still be recommended to use CerS or DEGS siRNA. This could prove that silencing of these genes in hepatocytes results in a lower ceramide expression in these cells.

This work can conclude that an in vitro liver targeting for the Apo E-LDLR pathway was established. This targeting indicates that a hepatocyte specific gene silencing could be used in the future to lower ceramide plasma levels and combat atherosclerosis. Further investigations using the recommendations could provide more insights and remove some of the mentioned uncertainties.

7 REFERENCES

1. Falk E. Pathogenesis of Atherosclerosis. J Am Coll Cardiol. 2006 Apr 18;47(8):C7–12.
2. Atherosclerosis - What Is Atherosclerosis? | NHLBI, NIH [Internet]. [cited 2023 May 22]. Available from: https://www.nhlbi.nih.gov/health/atherosclerosis
3. Badimon L, Vilahur G. Thrombosis formation on atherosclerotic lesions and plaque rupture. J Intern Med. 2014 Dec 1;276(6):618–32.
4. Kowara M, Cudnoch-Jedrzejewska A. Pathophysiology of Atherosclerotic Plaque Development-Contemporary Experience and New Directions in Research. Int J Mol Sci [Internet]. 2021 Apr 1 [cited 2023 May 22];22(7). Available from: /pmc/articles/PMC8037897/
5. Zhang J, Zu Y, Dhanasekara CS, Li J, Wu D, Fan Z, et al. Detection and Treatment of Atherosclerosis Using Nanoparticles. Wiley Interdiscip Rev Nanomed Nanobiotechnol [Internet]. 2017 Jan 1 [cited 2023 May 22];9(1). Available from: /pmc/articles/PMC5133203/
6. Bentzon JF, Otsuka F, Virmani R, Falk E. Mechanisms of Plaque Formation and Rupture. Circ Res [Internet]. 2014 Jun 19 [cited 2023 May 22];114(12):1852–66. Available from: https://www.ahajournals.org/doi/abs/10.1161/CIRCRESAHA.114.302721
7. Zorginstituut Nederland. statinen [Internet]. [cited 2023 May 22]. Available from: https://www.farmacotherapeutischkompas.nl/bladeren/groepsteksten/statinen
8. Atherosclerosis - Treatment | NHLBI, NIH [Internet]. [cited 2023 May 22]. Available from: https://www.nhlbi.nih.gov/health/atherosclerosis/treatment
9. Choi RH, Tatum SM, Symons JD, Summers SA, Holland WL. Ceramides and other sphingolipids as drivers of cardiovascular disease. Nat Rev Cardiol [Internet]. 2021 Oct 1 [cited 2023 May 26];18(10):701. Available from: /pmc/articles/PMC8978615/
10. Shu H, Peng Y, Hang W, Li N, Zhou N, Wang DW. Emerging Roles of Ceramide in Cardiovascular Diseases. Aging Dis [Internet]. 2022 Feb 1 [cited 2023 May 26];13(1):232. Available from: /pmc/articles/PMC8782558/
11. Zabielski P, Urszula Błachnio-Zabielska A, Wó Jcik B, Chabowski A, Gó Rski J. Effect of plasma free fatty acid supply on the rate of ceramide synthesis in different muscle types in the rat. 2017;

12. Ruangsiriluk W, Grosskurth SE, Ziemek D, Kuhn M, Des Etages SG, Francone OL. Silencing of enzymes involved in ceramide biosynthesis causes distinct global alterations of lipid homeostasis and gene expression. J Lipid Res [Internet]. 2012 Aug 1 [cited 2023 May 30];53(8):1459–71. Available from: http://www.jlr.org/article/S0022227520418504/fulltext
13. Schmidt S, Gallego SF, Zelnik ID, Kovalchuk S, Albæk N, Sprenger RR, et al. Silencing of ceramide synthase 2 in hepatocytes modulates plasma ceramide biomarkers predictive of cardiovascular death. Mol Ther [Internet]. 2022 Apr 6 [cited 2023 May 30];30(4):1661–74. Available from: https://pubmed.ncbi.nlm.nih.gov/34400330/
14. Kulkarni JA, Witzigmann D, Thomson S, Chen THH, Leavitt BR, Cullis PR, et al. The current landscape of nucleic acid therapeutics. Nature Nanotechnology [Internet]. 2021 May 31;16(6):630–43. Available from: https://doi.org/10.1038/s41565-021-00898-0
15. Sridharan K, Gogtay NJ. Therapeutic nucleic acids: current clinical status. Br J Clin Pharmacol. 2016;659–72.
16. Dana H, Mahmoodi Chalbatani G, Mahmoodzadeh H, Karimloo R, Rezaiean O, Moradzadeh A, et al. Molecular Mechanisms and Biological Functions of siRNA. Int J Biomed Sci www.ijbs.org 48 INTERNATIONAL JOURNAL of BIOMEDICAL SCIENCE [Internet]. 2017 [cited 2023 May 30];13(2). Available from: www.ijbs.org
17. Tenchov R, Bird R, Curtze AE, Zhou Q. Lipid Nanoparticles From Liposomes to mRNA Vaccine Delivery, a Landscape of Research Diversity and Advancement. 2021 [cited 2023 May 30]; Available from: https://doi.org/10.1021/acsnano.1c04996
18. Evers MJW, Kulkarni JA, van der Meel R, Cullis PR, Vader P, Schiffelers RM. State-of-the-Art Design and Rapid-Mixing Production Techniques of Lipid Nanoparticles for Nucleic Acid Delivery. Vol. 2, Small Methods. John Wiley and Sons Inc; 2018.
19. Eygeris Y, Gupta M, Kim J, Sahay G. Chemistry of Lipid Nanoparticles for RNA Delivery. Acc Chem Res [Internet]. 2022 Jan 4 [cited 2023 Apr 16];55(1):2–12. Available from: https://pubs.acs.org/doi/abs/10.1021/acs.accounts.1c00544

20. Varkouhi AK, Scholte M, Storm G, Haisma HJ. Endosomal escape pathways for delivery of biologicals. Journal of Controlled Release. 2011 May 10;151(3):220–8.
21. Yu B, Wang X, Zhou C, Teng L, Ren W, Yang Z, et al. Insight into Mechanisms of Cellular Uptake of Lipid Nanoparticles and Intracellular Release of Small RNAs. Pharm Res. 2014 May;31.
22. Zalba S, ten Hagen TLM, Burgui C, Garrido MJ. Stealth nanoparticles in oncology: Facing the PEG dilemma. Journal of Controlled Release. 2022 Nov 1;351:22–36.
23. Regen SL. Cholesterol's Condensing Effect: Unpacking a Century-Old Mystery. JACS Au [Internet]. 2022 Jan 1 [cited 2023 Apr 16];2(1):84. Available from: /pmc/articles/PMC8791060/
24. Kularatne RN, Crist RM, Stern ST. The Future of Tissue-Targeted Lipid Nanoparticle-Mediated Nucleic Acid Delivery. Pharmaceuticals [Internet]. 2022 Jul 1 [cited 2023 May 30];15(7). Available from: /pmc/articles/PMC9322927/
25. Böttger R, Pauli G, Chao PH, Fayez N AL, Hohenwarter L, Li SD. Lipid-based nanoparticle technologies for liver targeting. 2020 [cited 2023 May 30]; Available from: https://doi.org/10.1016/j.addr.2020.06.017
26. Carr ESRM. Ceramides' role in liver disease. www.asbmb.org [Internet]. 2021 May 5; Available from: https://www.asbmb.org/asbmb-today/science/050521/ceramides-role-in-liver-disease
27. Sebastiani F, Yanez Arteta M, Lerche M, Porcar L, Lang C, Bragg RA, et al. Apolipoprotein E Binding Drives Structural and Compositional Rearrangement of mRNA-Containing Lipid Nanoparticles. 2021 [cited 2023 May 31]; Available from: https://doi.org/10.1021/acsnano.0c10064
28. Huang Y, Mahley RW. Apolipoprotein E: Structure and Function in Lipid Metabolism, Neurobiology, and Alzheimer's Diseases. Neurobiol Dis [Internet]. 2014 Dec 1 [cited 2023 May 30];72PA(Part A):3. Available from: /pmc/articles/PMC4253862/
29. Sato Y, Kinami Y, Hashiba K, Harashima H. Different kinetics for the hepatic uptake of lipid nanoparticles between the apolipoprotein E/low density lipoprotein receptor and the N-acetyl-d-galactosamine/asialoglycoprotein receptor pathway. Journal of Controlled Release. 2020 Jun 10;322:217–26.

30. Go GW, Mani A. Low-density lipoprotein receptor (LDLR) family orchestrates cholesterol homeostasis. PubMed [Internet]. 2012 Mar 29; Available from: https://pubmed.ncbi.nlm.nih.gov/22461740
31. Tanowitz M, Hettrick L, Revenko A, Kinberger GA, Prakash TP, Seth PP. Asialoglycoprotein receptor 1 mediates productive uptake of N-acetylgalactosamine-conjugated and unconjugated phosphorothioate antisense oligonucleotides into liver hepatocytes. Nucleic Acids Res [Internet]. 2017 [cited 2023 May 30];45(21):12388–400. Available from: https://academic.oup.com/nar/article/45/21/12388/4561646
32. Springer AD, Dowdy SF. GalNAc-siRNA Conjugates: Leading the Way for Delivery of RNAi Therapeutics. [cited 2023 May 30]; Available from: www.liebertpub.com
33. Weingärtner A, Bethge L, Weiss L, Sternberger M, Lindholm MW. Less Is More: Novel Hepatocyte-Targeted siRNA Conjugates for Treatment of Liver-Related Disorders. [cited 2023 May 30]; Available from: https://doi.org/10.1016/j.omtn.2020.05.026.
34. Akinc A, Querbes W, De S, Qin J, Frank-Kamenetsky M, Jayaprakash KN, et al. Targeted delivery of RNAi therapeutics with endogenous and exogenous ligand-based mechanisms. Molecular Therapy. 2010;18(7):1357–64.
35. Malvern Panalytical. Dynamic Light Scattering: An Introduction in 30 Minutes. Malvern Panalytical [Internet]. 2021 Sep 18; Available from: https://www.malvernpanalytical.com/en/learn/knowledge-center/technical-notes/TN101104DynamicLightScatteringIntroduction
36. Stetefeld J, McKenna SA, Patel TR. Dynamic light scattering: a practical guide and applications in biomedical sciences. Biophys Rev [Internet]. 2016 Dec 1 [cited 2023 Apr 8];8(4):409. Available from: /pmc/articles/PMC5425802/
37. Danaei M, Dehghankhold M, Ataei S, Hasanzadeh Davarani F, Javanmard R, Dokhani A, et al. Impact of Particle Size and Polydispersity Index on the Clinical Applications of Lipidic Nanocarrier Systems. Pharmaceutics [Internet]. 2018 May 18 [cited 2023 May 8];10(2). Available from: /pmc/articles/PMC6027495/
38. Quant-itTM RiboGreen RNA Assay Kit and RiboGreen RNA Reagent, RediPlateTM 96 RiboGreenTM RNA Quantitation Kit | Thermo Fisher Scientific

- BE [Internet]. [cited 2023 May 25]. Available from: https://www.thermofisher.com/order/catalog/product/R11490
39. Schwartz K, Bochkariov D. Novel chemiluminescent Western blot blocking and antibody incubation solution for enhanced antibody-antigen interaction and increased specificity. Electrophoresis [Internet]. 2017 Oct 1 [cited 2023 May 25];38(20):2631–7. Available from: https://onlinelibrary.wiley.com/doi/full/10.1002/elps.201700143
40. Dot blot protocol | Abcam [Internet]. [cited 2023 May 5]. Available from: https://www.abcam.com/protocols/dot-blot-protocol
41. Detection of Glycoproteins Using Lectins in Histochemistry, ELISA, and Western Blot Applications [Internet]. Vector Laboratories. Available from: https://vectorlabs.com/wp-content/uploads/2023/01/VL_LIT3055_Detect.Glycoproteins_SuppProtocol.LBL02552.pdf
42. Culture Collections. Culture Collections [Internet]. [cited 2023 Apr 19]. Available from: https://www.culturecollections.org.uk/news/ecacc-news/sticky-issues-with-293-cells.aspx
43. 0.1% Gelatin Solution - PCS-999-027 | ATCC [Internet]. [cited 2023 Apr 19]. Available from: https://www.atcc.org/products/pcs-999-027
44. McKinnon KM. Flow Cytometry: An Overview. Curr Protoc Immunol [Internet]. 2018 Feb 2 [cited 2023 May 22];120:5.1.1. Available from: /pmc/articles/PMC5939936/
45. Flow Cytometry (FACS) Fluorescence Measurement | Sino Biological [Internet]. [cited 2023 May 22]. Available from: https://www.sinobiological.com/category/fcm-facs-fluorescence-measurement
46. A practical guide for use of PE and APC in flow cytometry | AAT Bioquest [Internet]. [cited 2023 May 26]. Available from: https://www.aatbio.com/resources/assaywise/2017-6-2/a-practical-guide-for-use-of-pe-and-apc-in-flow-cytometry
47. Spectrum [FITC (Fluorescein-5-isothiocyanate)] | AAT Bioquest [Internet]. [cited 2023 May 26]. Available from: https://www.aatbio.com/fluorescence-excitation-emission-spectrum-graph-viewer/5_fitc_fluorescein_5_isothiocyanate

48. Mahmood T, Yang PC. Western Blot: Technique, Theory, and Trouble Shooting. N Am J Med Sci [Internet]. 2012 Sep [cited 2023 May 25];4(9):429. Available from: /pmc/articles/PMC3456489/
49. Basic Principles of RT-qPCR | Thermo Fisher Scientific - BE [Internet]. [cited 2023 May 25]. Available from: https://www.thermofisher.com/be/en/home/brands/thermo-scientific/molecular-biology/molecular-biology-learning-center/molecular-biology-resource-library/spotlight-articles/basic-principles-rt-qpcr.html
50. What is qPCR? | Ask a Scientist [Internet]. [cited 2023 May 26]. Available from: https://www.thermofisher.com/blog/ask-a-scientist/what-is-qpcr/
51. Bustin SA, Benes V, Nolan T, Pfaffl MW. Quantitative real-time RT-PCR – a perspective. J Mol Endocrinol [Internet]. 2005 Jun 1 [cited 2023 May 26];34(3):597–601. Available from: https://jme.bioscientifica.com/view/journals/jme/34/3/0340597.xml
52. Cell Preparation for Flow Cytometry Research Use Only. [cited 2023 May 5]; Available from: http://www.tissuedissociation.com
53. Flow cytometry (FACS) staining protocol (Cell surface staining). Yale Flow Cytometry [Internet]. [cited 2023 May 5]. Available from: https://medicine.yale.edu/immuno/flowcore/protocols/analysis/
54. BestProtocols: Staining Cell Surface Targets for Flow Cytometry | Thermo Fisher Scientific - BE [Internet]. [cited 2023 May 5]. Available from: https://www.thermofisher.com/be/en/home/references/protocols/cell-and-tissue-analysis/protocols/staining-cell-surface-targets-flow-cytometry.html
55. Lectins: Wheat Germ Agglutinin (WGA), succinylated, Fluorscein labeled [Internet]. [cited 2023 May 5]. Available from: https://vectorlabs.com/products/glycobiology/fluorescein-succinylated-wheat-germ-agglutinin
56. PE Mouse Anti-ASGPR 1 [Internet]. [cited 2023 May 22]. Available from: https://www.bdbiosciences.com/en-au/products/reagents/flow-cytometry-reagents/research-reagents/single-color-antibodies-ruo/pe-mouse-anti-asgpr-1.563655
57. Yan H, Ma Y, Gui YZ, Wang S, Wang X, Gao F, et al. MG132, a proteasome inhibitor, enhances LDL uptake in HepG2 cells in vitro by regulating LDLR and

PCSK9 expression. Acta Pharmacologica Sinica [Internet]. 2014 Jul 21;35(8):994–1004. Available from: https://doi.org/10.1038/aps.2014.52

8 ANNEX

Table 8.1: NanoAssembler settings for the priming and flushing of the cartridge and the formulation of the LNPs

Variabels	Priming and flushing	Formulation
Flow rate ratio	1:1 (aqueous to ethanol)	3:1 (aqueous to ethanol)
Total flow rate	12 mL/min	9 mL/min
Start waste volume	0.350 mL	0.150 mL
End waste volume	0.050 mL	0.020 mL

Table 8.2: Sequences of the used primers for the RT-qPCR analysis

Primer	Sequence
GAPDH[a] human paper Fw[b]	5'-TCAAGGCTGAGAACGGGAAG
GAPDH human paper Rv[c]	5'-CGCCCACTTGATTTTGGAG
Beta-actin human Fw	5'-CCTTGCACATGCCGGAG
Beta-actin human Rv	5'-ACAGAGCCTCGCCTTTG
AR[d] human Fw	5'-GTAACTACCCGAGCATGGC
AR human Rv	5'-CCCCTTGTAGTGGGTCAAAC

[a] GAPDH: glyceraldehyde-3-phosphate dehydrogenase

[b] Fw: foward

[c] Rv: reverse

[d] AR: androgen receptor

Master dissertation submitted to the faculty of Pharmaceutical Sciences, performed in collaboration with the Central Diagnostic Laboratory University Medical Center Utrecht

Promotor: Prof. dr. Koen Raemdonck

Second promotor: Prof. dr. Raymond Schiffelers

Supervisor: Head Technician Arnold Koekman

Commissioners: Prof. dr. Stefaan De Smedt and Dr. Karen Peynshaert

This master dissertation is an examination document that not necessarily has been corrected for eventual mistakes. The information, conclusions and points of view in this master dissertation are those of the author and do not necessarily represent the opinion of the promoter or his/her research group.